SIMULATION OF MEMS HEAT EXCHANGER WITH VARIOUS WORKING FLUIDS

A thesis submitted by

NUSRAT JAHAN CHHANDA

In partial fulfilment of the requirements for the degree of

MASTER OF SCIENCE IN MECHANICAL ENGINEERING

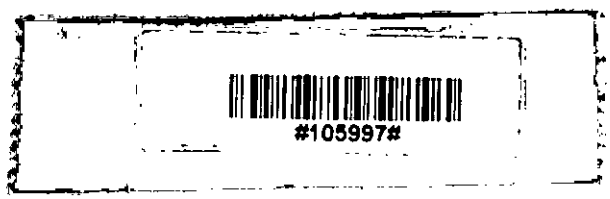

DEPARTMENT OF MECHANICAL ENGINEERING
BANGLADESH UNIVERSITY OF ENGINEERING & TECHNOLOGY
Dhaka 1000, Bangladesh

July 2008

The thesis titled **'SIMULATION OF MEMS HEAT EXCHANGER WITH VARIOUS WORKING FLUIDS',** submitted by Nusrat Jahan Chhanda, Roll No. 100510025F, Session October 2005, has been accepted as satisfactory in partial fulfilment of the requirement for the degree of **Master of Science in Mechanical Engineering** on July 26, 2008.

BOARD OF EXAMINERS

Dr. Maglub Al Nur
Professor
Department of Mechanical Engineering
BUET, Dhaka

Chairman
(Supervisor)

Dr. Abu Rayhan Md. Ali
Professor and Head
Department of Mechanical Engineering
BUET, Dhaka

Member
(Ex-officio)

Dr. Chowdhury Md. Feroz
Professor
Department of Mechanical Engineering
BUET, Dhaka

Member

Dr. A. K. M. Iqbal Hussain
Professor
Department of MCE
Islamic University of Technology (IUT), Gazipur

Member
(External)

TABLE OF CONTENTS

CANDIDATE'S DECLARATION

It is hereby declared that this thesis or any part of it has not been submitted elsewhere for the award of any degree or diploma.

Nusrat Jahan Chhanda

Nusrat Jahan Chhanda

ACKNOWLEDGEMENT

It is indeed a great pleasure and proud privilege for the author to express her deepest sense of sincere thanks and gratitude to her supervisor, Dr. Maglub Al Nur, Professor, Department of Mechanical Engineering, Bangladesh University of Engineering & Technology (BUET), Dhaka, for his supervision and untiring support that were a constant source of inspiration throughout this research work. The author owe to him for his continuous guidance and valuable suggestions without which this study would be difficult.

The author expresses her heartiest gratitude to Engr. Muhannad Mustafa, Department of Mechanical Engineering, BUET for his keen interest about the progress of this work. She also would like to thank her parents Mrs. Niger Sultana and Mr. M. A. Mannan and other family members, for their co-operation in the successful completion of this work.

LIST OF FIGURES

LIST OF TABLES

Nomenclature

Roman symbols:

A	Surface area (m^2)
A_1	Area of fluid entry (m^2)
A_2	Surface area of convection (m^2)
c_c	Specific heat at constant pressure of cold fluid (J/kg.K)
C_p	Specific heat at constant pressure (J/kg.K)
D_h	Hydraulic diameter (m)
h	Convective heat transfer coefficient ($W/m^2.K$)
k	Thermal conductivity (W/m.K)
$\dot{m}$	Mass flow rate (kg/s)
$\dot{m}_c$	Mass flow rate of cold fluid (kg/s)
n	Normal flow direction
Nu	Nusselt number
Q_{air}	Heat transfer in air (Watt)
Q_{conv}	Heat transfer due to convection (Watt)
q_{max}	Maximum possible heat transfer (Watt)
Re	Reynolds number
T_m	Bulk temperature (K)
T_{c_2}	Outlet temperature of cold fluid (K)
T_{c_1}	Inlet temperature of cold fluid (K)
T_h, T_w	Wall Temperature (K)
T_{h_1}	Inlet temperature of hot fluid (K)
$T_{h_{inlet}}$	Inlet temperature of hot fluid (K)
$T_{h_{outlet}}$	Outlet temperature of hot fluid (K)
T_i	Inlet Temperature (K)
T_0	Outlet mean temperature (K)
U_{av}	Average velocity (m/s)
u	Local velocity (m/s)
P	Pressure
Pr	Prandtl number

Greek symbols:

ε	Effectiveness (%)
μ	Dynamic viscosity (kg/m.s)
ρ	Density (kg/m^3)

Abbreviation:

CFD	Computational fluid dynamics
CPU	Central processing unit
MEMS	Microelectromechanical systems
MOO	Multi-objective optimisation
MST	Microsystems technology
NEMS	Nanoelectromechanical systems

Abstract

The introduction of MEMS heat exchanger has established a new era in the history of heat transfer in micro scale systems. This study is based on an analysis conducted using commercial finite element package. During the analysis different parameters such as temperature of wall, fluid inlet velocity and other fluid properties have been used as input parameters for solving the governing equations and boundary conditions. After solving the problem in finite element method, outlet mean temperature has been obtained which is then used for further calculation to evaluate heat transfer behaviour of fluids.

The aim of this simulation is to find a substitute of conventional working fluids used as coolant for MEMS heat exchanger and also to evaluate performance of fluids for different geometry. Usually water and air is more preferable as coolant for their low cost and availability. But they have some disadvantages too such as dust in content, forming rust in metal contact etc. So a second option is needed such that the conventional fluids can be substituted. Freon 11 has shown the highest outlet mean temperature during the study. Freon 113 and ammonia has also shown a good percentage of increment of heat transfer when surface area is increased. Moreover in this analysis, emphasis is also given on the effect of geometry on the performance of different fluids. It is apparent from this work that rectangular surface heat exchanger shows highest outlet mean temperature as well as heat transfer of fluids in comparison to other geometry. Therefore it may be suggested that rectangular surface may be used instead of wavy surface as it is also easy to manufacture.

This work is an extension of a tutorial which showed the calculation of outlet mean temperature of water for wavy surface MEMS heat exchanger with pitch 0.95 mm. The rest of the work done in this analysis is based on the need of evaluation of performance of fluids as well as geometry. The overall results obtained from this work are quite satisfactory. It is thought to be helpful for the researchers in this field.

Chapter 1

Introduction

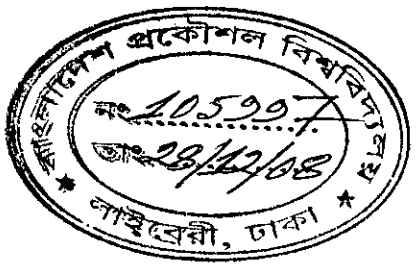

1.1 Introduction

Microelectromechanical systems (MEMS) is the technology of the very small, and merges at the nano-scale into nanoelectromechanical systems (NEMS) and nanotechnology. Heat exchangers are mostly used in processes to remove heat when convective cooling from fans and fins are not enough. For having the advantage of superior heat exchange properties, compact design at industrial throughput and low inner volume, the micro heat exchangers are becoming increasingly popular in the fields of chemical, electronic and aerospace industries. In the chemical processing industries, micro heat exchangers have been used as fuel processors, combustors and evaporators. One of the very common uses of Micro Heat Exchangers is for the cooling of electronic equipment. The use of MEMS-fabricated micro-channels for heat absorption and removal from microelectronic devices is thermally efficient due to the large surface area available for heat exchange. The use of MEMS devices in aerospace systems is expected to be highly application specific and would typically aim to reduce size, weight, and power consumption at the component level. These systems are already in use in several avionic applications. In space applications, miniaturised actuators in addition to miniaturised sensor systems play an important role. The cost advantage and electronic integration capabilities of MEMS enable the feasibility of distributed measurement and actuation. Nevertheless, microsystems technology is considered a key technology for future satellites and launch vehicles as the attributes of low mass, volume and power consumption are key issues to reducing the cost of access to space.

The latest generation of gigahertz-clock-rate RISC and CISC CPUs is becoming more challenging to fit into designs. These chips are squeezing into smaller and smaller spaces with very little place for heat to escape. Total power-dissipation levels are now around

110 W, and peak power densities are reaching 400 to 500 W/mm^2 and are constantly on the increase. As a result, higher performance and greater reliability levels are extremely tough to attain. Until now, the solution was to use active heat sinks and passive fluid heat pipes. These types of structures are costly and bulky, and they take up too much real estate on the pc board. The heat sink can be some 3000 times larger than the CPU it is cooling. A standard 120-W Intel Pentium 4 microprocessor generally uses a heat sink that dwarfs the CPU hotspot that it's trying to cool.

Microelectromechanical-systems (MEMS) heat exchangers have found some success here, but the key missing element has been a practical means of removing the heat. The Pentium 4 currently consumes about 82 W. This figure will climb with time. As a possible solution micro channel with fluid cooling media can be employed as providing very high heat-transfer coefficient. Although such systems are being already constructed their performance is still far from being quite satisfactory and a lot of research efforts have to be done to solve the existing problems.

In the present research, a two dimensional model is developed for investigation of MEMS heat exchanger with various working fluids and different surface geometry. The heat exchanger is modeled by stacking several square plates on top of each other whilst leaving a gap of 1 mm in between. The length of the plates is maintained as 9.5 mm. As the knowledge of effect of different working fluids on heat transfer behaviour in different geometry is far from being complete, this research gives emphasis on evaluation of the performance of MEMS heat exchanger with micro channels of different shape for different working fluids.

1.2 Objective of the Present Research

The inspiration of this work is achieved from a tutorial given in built-in finite element package which shows the way of calculation of outlet mean temperature using this package. As most of the previous researches is based on wavy shape and air as working fluid so this work is an attempt of evaluating the performance of different fluids such as

water , Freon 113, Freon 11 and ammonia for different geometry such as plain, wavy , triangular and rectangular surface MEMS heat exchanger.

The specific objectives of the present research work are as follows:

(a) Evaluation of performance of MEMS heat exchanger using various working fluids through micro channels with different geometry within a particular temperature range.

(b) Determination of optimum conditions for various working fluids in MEMS heat exchanger for various engineering applications.

(c) Comparison of the results obtained from present work with the results available in the literature.

The results are expected to be useful as a possible solution for microchannel-based circuits with cooling media and many other practical applications of this kind.

1.3 Outline of the Thesis

This thesis consists of five chapters. The entire work is based on simulation and computation.

Chapter 1 gives a background of this research work and defines the purpose and directions of investigation.

Chapter 2 depicts some of the previous research works relevant to this topic.

Chapter 3 demonstrates a model used for simulation by finite element method. As the simulation results are satisfactorily validated by the available literature, the model is used for further investigation to obtain a good understanding of effect of different working fluids on heat transfer behaviour in micro heat exchanger.

Chapter 4 presents results and discussion obtained from simulation.

In Chapter 5 outcome of the research work has been summarized.

Chapter 2

Literature Review

Fast development of microelectronic circuits led the modern researchers to carry out researches in the fluid flow and heat transfer characteristics in micro channels. In 1998, Yuen and Hsu [1] designed and fabricated a micro-channel heat exchanger, the important basic component of a microminiature Joule-Thomson cryogenic refrigerator. Preliminary experiments showed that the heat exchanger is mechanically robust and has excellent thermal performance characteristics. A computer code was developed both to interpret the performance characteristics of the heat exchanger and to serve as a design tool for the refrigerator. Results of numerical simulation showed that the micro-channel heat exchanger is effective in generating a uniform liquid fraction over the whole base surface. Thus the design objective of generating a uniform temperature surface was met. Hardt *et al.* [2] found that channels equipped with micro fins allow for a rapid exchange of heat. Such designs exhibit a potential to construct very compact heat exchangers and lend themselves as components of heat-exchanger reaction systems. The numerical results clearly showed a superior performance of the reactor containing microstructured heat-exchanger channels compared to unstructured channels.

Okabe *et al.* [3] built up the optimization flow for Micro Heat Exchanger with the commercial multi-physics solver and pointed out the necessary functionalities of the commercial solver to be used in the field of evolutionary computation. The purpose of their work was to optimise a micro heat exchanger using Multi-Objective Optimisation (MOO). The physical phenomenon in micro heat exchanger is multidisciplinary and involves conjugate heat transfer. In order to solve the conjugate heat transfer problem, they used a commercial computational fluid dynamics (CFD) solver called *CFD-ACE+* developed by Computational Fluids Dynamics Research Corporation in the USA. This CFD solver was interfaced with their in-house developed evolutionary algorithms.

Hossain and Islam [4] solved two-dimensional Navier -Stokes and energy equations numerically for unsteady laminar flow in periodic wavy (sinusoidal and triangular) channels. The flow in the channels has been observed to be steady up to a critical Reynolds number. They found that beyond the critical Reynolds number the flow becomes self sustained. Chandratilleke *et al.* [5] developed Simulation models for the micro-heat exchanger to assess the influence of critical system variables on heat transfer rates and pumping power, and to ascertain optimal parametric combinations for thermoelectric applications. With appropriate selection of operating parameters, this micro-heat exchanger design offered thermal resistances of the order 0.01-0.02 K/W and low fluid pump powers.

McCandless *et al.* [6] and Li [7] showed cooling performance of micro-machined MEMS Heat Exchanger in their work. McCandless et al. demonstrated heat exchangers and catalytic reactors with micro-scaled features can provide significant weight and volume reductions compared to other available systems. They reported on development of micro-machined thermal and chemical devices that have surface features of the order of 100's of microns, over areas of the order of 10's to 100's of cm. They have also reported on the performance of micro-machined cross-flow heat exchangers with a performance to volume ratio which is 10 times higher than the best heat exchanger available. The main advantage of small heat exchangers is their high cooling performance. Li [7] showed that it may be even up to 60 times higher than the corresponding values for conventional, macroscale heat exchangers.

Morimoto *et al.* [8] made a series of numerical simulation of the flow and heat transfer in modeled counter-flow heat exchangers with oblique wavy walls for optimal shape design of recuperators. They found that the flow field is drastically modified due to the counter-rotating streamwise vortices induced by the wavy walls. Moreover, with the oblique angle of 50-60 degree, significant heat transfer enhancement is achieved at the cost of relatively small pressure loss.

Mébrouk *et al.* [9] reported a numerical investigation of natural convection and fluid flow in a horizontal wavy enclosed. Its bottom wall was varied with a sinusoidal function while the top and the two side walls were flat. Their numerical results showed that the flow and the heat transfer are strongly affected by the amplitude of the sinusoidal profile. Eiamsa-ard and Promvonge [10] performed an experimental study on a helical-tape insert in a circular wavy-surfaced tube using hot air as the test fluid. The influence of the helical tape insert on the heat transfer and pressure drop characteristics had been demonstrated. They showed that the increases in heat transfer and pressure drop are strongly influenced by turbulence/swirling motion induced by the helical-tape and wavy-surfaced wall. As the Reynolds number increases, the turbulence/swirling flow is stronger which in turn results in an increase in the heat transfer and pressure drop. The maximum increases in heat transfer rate and pressure drop are found to be about 2.67 and 22.3 times the plain tube for the flow range studied.

Davis *et al.* [11] discussed the major design issues for commercial CPU coolers in their study. Their paper presents descriptions of low thermal resistance heat exchangers for CPU cooling and thermoelectric system designs for a more advanced cooling capacity. They used an experimental setup to test the efficacy of the waterblocks in a typical CPU cooling environment. They found that water-cooling solutions overcome both conduction resistance & airflow limitations, and therefore allow another generation of die size decreases & CPU power increases.

As it can be seen from the above literatures, although many research works regarding micro heat exchangers are available and successful applications have been reported, the variation of performance with different working fluids had rarely been carried out. This research reports the comparison among working fluids when these are used in MEMS heat exchanger under two dimensional steady state condition.

Chapter 3

Model Definition

3.1 Introduction

MEMS-Electro-Mechanical Systems (MEMS) is the technology which integrates mechanical elements, sensors, actuators and electronics into complex micrometer-sized machines--also referred to as micromachines and microsystems technology (MST). MEMS are made up of components between 1 to 100 micrometers in size (i.e. 0.001 to 0.1 mm) and MEMS devices generally range in size from 20 micrometers (20 millionth of a meter) to a millimeter. Heat exchangers are used to transfer heat from one medium to another. These can both cool and heat fluids and solid materials. MEMS heat exchangers are heat exchangers in which (at least one) fluid flows in lateral confinements with typical dimensions below 1 mm.

3.2 Description of the Model

Figure 3.1 (a) depicts a section of the heat exchanger which is considered for the present analysis. It is constructed by stacking several square plates of sinusoidal shape on top of each other whilst leaving a gap in between. To simplify the modeling, only a cross section between two plates is considered (shown in Figure 3.2 where A1 denotes area of fluid entry and A2 represents the surface area of convection). The distance between two plates is maintained at 1 mm while the linear length of the plate is 9.5 mm. Fluid is used as coolant to transfer heat which circulates in gaps between the corrugated wavy walls. Walls are considered as isothermal surfaces. At the inlet, developed fluid flow with a parabolic shape of velocity profile is assumed. It is also assumed that fluids enter through the wavy surfaces with a definite temperature. Along the wavy surfaces no-slip condition is assumed as boundary condition. Finally, at the outlet or outflow boundary, normal flow

(perpendicular flow) velocity conditions and convective flux heat transfer are assumed. Heat is removed from the heated wall and transferred to the coolant. At the outlet, velocity weighted mean temperature is obtained.

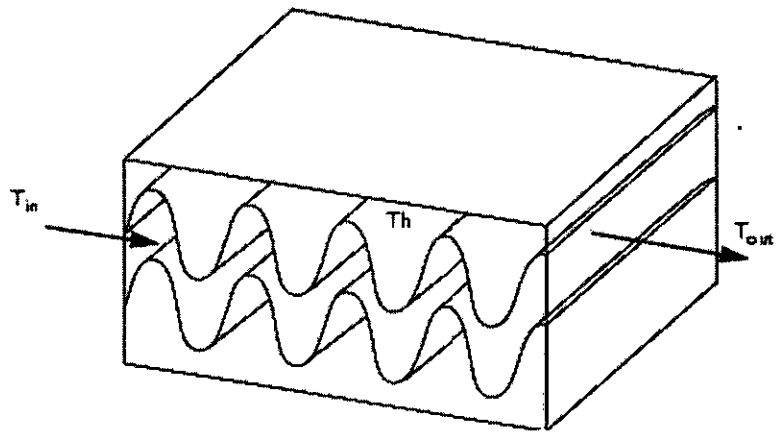

Figure 3.1 MEMS Heat Exchanger Geometry

The overall performance of the heat exchanger is calculated from the outlet mean temperature of the working fluids. For heat transfer medium four different fluids are used to evaluate their performances, these are: water, ammonia, Freon-11 and Freon-113 for a particular temperature range. The operating temperature range spans from 48 to 90 °C (321 K to 363 K). At this temperature range, only water remains in liquid phase (boiling point 100°C), other working fluids such as ammonia, Freon 113 and Freon 11 remain in vapor phase. The boiling point of R-11 at atmospheric pressure is 23.77°C. Boiling point of R-113 and ammonia is 47.6°C and -33.3°C respectively at atmospheric pressure [14]. The temperature range is chosen such that only single phase flow of working fluids can occur in the heat exchanger.

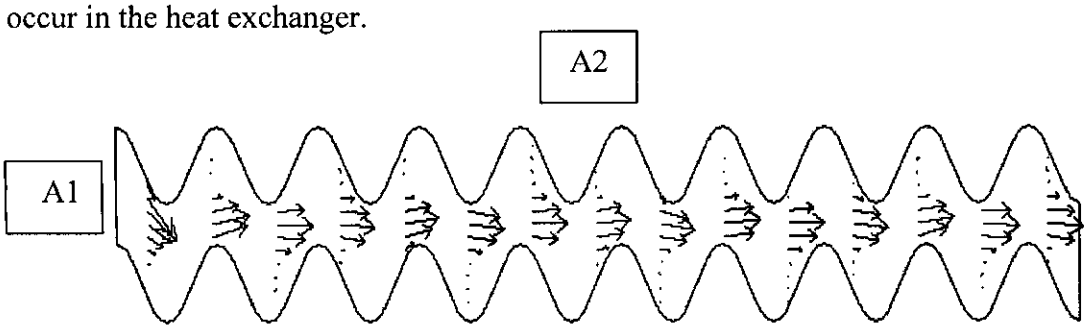

Figure 3.2 Cross section of the Fluid Flow Field

The analysis is done by varying the velocity and properties of fluids as well as the pitch. Pitch can be defined as the distance between two adjacent peaks and it is calculated as linear length of the plate divided by total number of peaks. The performance of a MEMS heat exchanger for a particular fluid changes by varying the pitches.

The initial length and distance between the two plates are maintained constant throughout the investigation while varying the pitch. The number of peaks per unit length is increased. As a consequence, the pitch reduces from a value of 0.95 mm to 0.11875 mm. In the present work, analysis has been done for the heat transfer behaviour between plain surface and wavy surface heat exchangers. In case of wavy surface MEMS heat exchanger, investigations have been conducted for four different pitches.
The values of four different pitches for wavy surfaces and the ratio of A1 and A2 for wavy surface and plain surface are shown in Table 3.1

Table 3.1 Values of A1/A2 for Different Surfaces

Surface Type	**A1/A2**
Plain	0.105
Wavy -Pitch 0.95 mm	0.0476
Wavy -Pitch 0.475 mm	0.0371
Wavy -Pitch 0.2375 mm	0.0231
Wavy -Pitch 0.11875 mm	0.0114
Triangle -Pitch 0.95 mm	0.066
Triangle -Pitch 0.475 mm	0.0403
Triangle -Pitch 0.2375 mm	0.0222
Triangle -Pitch 0.11875 mm	0.0114
Rectangle -Pitch 0.95 mm	0.05015
Rectangle -Pitch 0.475 mm	0.03289
Rectangle -Pitch 0.2375 mm	0.01949
Rectangle -Pitch 0.11875 mm	0.0107

Profiles of various types of MEMS heat exchangers investigated in this research are shown in Figure 3.3.

MEMS heat exchanger with plain surface

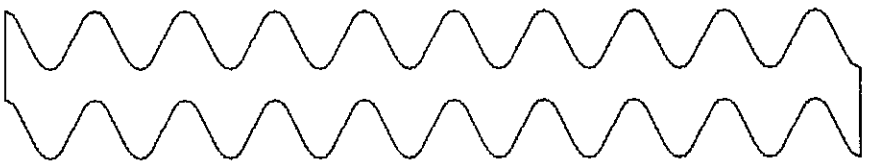

MEMS heat exchanger with wavy surface of pitch length 0.95 mm

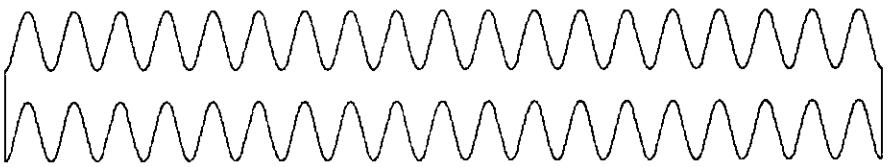

MEMS heat exchanger with wavy surface of pitch length 0.475 mm

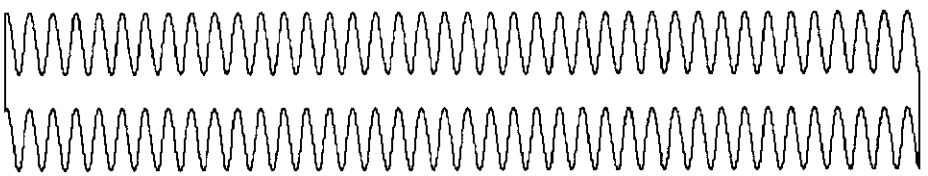

MEMS heat exchanger with wavy surface of pitch length 0.2375 mm

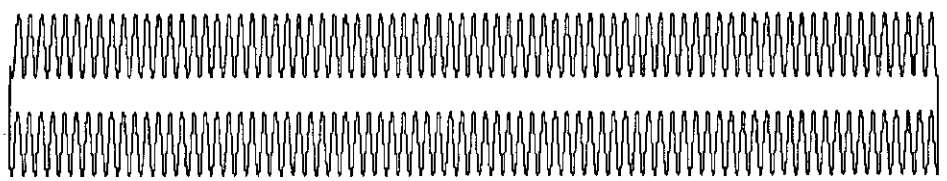

MEMS heat exchanger with wavy surface of pitch length 0.11875 mm

Figure 3.3 MEMS heat exchanger of plain and wavy surface

Triangular Surface

(a) Triangle surface of pitch length 0.95 mm

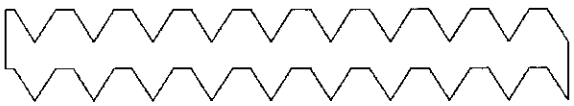

(b) Triangle surface of pitch length 0.475 mm

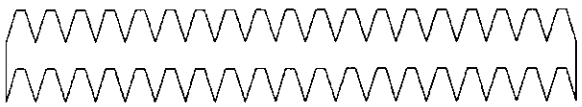

(c) Triangle surface of pitch length 0.2375 mm

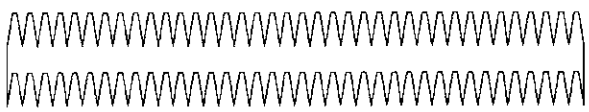

(d) Triangle surface of pitch length 0.11875 mm

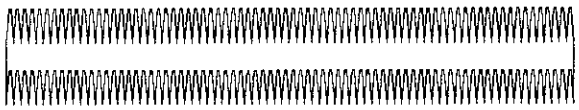

Rectangular Surface

(a) Rectangle surface of pitch length 0.95 mm

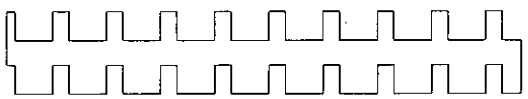

(b) Rectangle surface of pitch length 0.475 mm

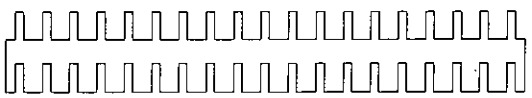

(c) Rectangle surface of pitch length 0.2375 mm

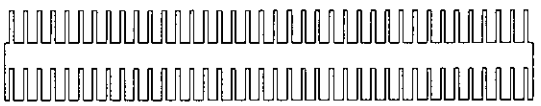

(d) Rectangle surface of pitch length 0.11875 mm

Figure 3.4 MEMS heat exchanger of triangular and rectangular surface

3.3 Governing Equations and Boundary Conditions

The governing equations in this system are the incompressible Navier-Stokes equation (Eq. 1) and continuity equation (Eq. 2) accounting for the motion of the fluid

$$\rho\left(\frac{\partial u}{\partial t}+u\frac{\partial u}{\partial x}+v\frac{\partial u}{\partial y}+w\frac{\partial u}{\partial z}\right)=\rho g_x-\frac{\partial p}{\partial x}+\mu\left(\frac{\partial^2 u}{\partial x^2}+\frac{\partial^2 u}{\partial y^2}+\frac{\partial^2 u}{\partial z^2}\right) \quad (1)$$

$$\frac{\partial u}{\partial x}+\frac{\partial v}{\partial y}+\frac{\partial w}{\partial z}=0 \quad (2)$$

and the convection and conduction equation (Eq. 3), without any heat sources, for the energy transport within the fluid

$$\frac{\partial^2 T}{\partial x^2}+\frac{\partial^2 T}{\partial y^2}+\frac{\partial^2 T}{\partial z^2}=\frac{\rho c_p}{k}\frac{\partial T}{\partial t} \quad (3)$$

For two dimensional analysis Equation 1, 2 and 3 can be simplified in following way,

$$\rho\left(\frac{\partial u}{\partial t}+u\frac{\partial u}{\partial x}+v\frac{\partial u}{\partial y}\right)=\rho g_x-\frac{\partial p}{\partial x}+\mu\left(\frac{\partial^2 u}{\partial x^2}+\frac{\partial^2 u}{\partial y^2}\right) \quad (4)$$

$$\frac{\partial u}{\partial x}+\frac{\partial v}{\partial y}=0 \quad (5)$$

$$\frac{\partial^2 T}{\partial x^2}+\frac{\partial^2 T}{\partial y^2}=\frac{\rho c_p}{k}\frac{\partial T}{\partial t} \quad (6)$$

The results are obtained in FEMLAB by solving Equation 4, 5 and 6 simultaneously in finite element method.

At the inlet, a parabolic velocity profile with a known constant temperature is specified. The analytical solution for a fully developed laminar flow profile between two parallel plates at a distance of 2B from each other is

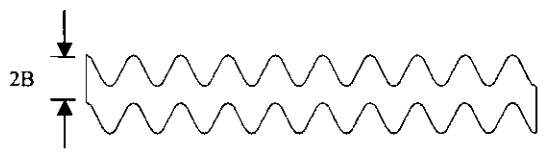

Thus the boundary condition is given as,

$$u = \frac{3}{2} U_{av} \left[1 - \left(\frac{x}{B} \right)^2 \right]$$

Here u is the local velocity and U_{av} is the average velocity.

Boundary condition for heat transfer at the inlet will be $T = T_{in}$

The walls have no-slip conditions for velocity and a specified temperature condition for the energy balance:

$u = 0$

$T = T_h$

Finally, at the outlet or outflow boundary, normal flow (perpendicular flow) velocity conditions and convective flux heat transfer are assumed:

$u.\ t = 0$

$p = 0$

$-k \nabla T.\ n = 0$

3.4 Expressions for Fluid Properties

For solving the governing equations, the values of different fluid properties have been given as input parameters in the Subdomain Expressions dialog box of FEMLAB. Fluid properties vary with temperature. So temperature dependent equations have been formed by using data given in Appendix A.

The expressions used in this analysis for different properties of different fluids are as follows:

for water

Dynamic viscosity= $0.11021-9.386\times10^{-4}\times T+2.684\times10^{-6}\times T^2-2.569\times10^{-9}\times T^3$

Specific heat at constant pressure = $4190.86-0.977\times T+0.019\times T^2-5.6e-5\times T^3$

Density = $757.3-0.0035\times T^2+1.8512\times T$

Thermal conductivity = $-(0.5841-0.0065\times T+8\times10^{-06}\times T^2)$

for Freon 11

Dynamic viscosity= $5\times10^{-06}+3\times10^{-11}\times T^2+1\times10^{-08}\times T$

Specific heat at constant pressure = $305.1-4\times10^{-05}\times T^2+0.8296\times T$

Density = $294.66+0.0044\times T^2-2.2953\times T$

Thermal conductivity = 0.008318

for Freon 113

Dynamic viscosity= $3\times10^{-06}-6\times10^{-12}\times T^2+3\times10^{-08}\times T$

Specific heat at constant pressure = $1257.8-4\times10^{-05}\times T^3+0.0317\times T^2-8.1821\times T$

Density = $-(99.231-1.3167\times T-9\times10^{-06}\times T^3+0.0058\times T^2)$

Thermal conductivity = 0.007798

For ammonia

Dynamic viscosity= $2\times10^{-05}+3\times10^{-10}\times T^2-1\times10^{-07}\times T$

Specific heat at constant pressure = $1990.2+0.0024\times T^2-0.2027\times T$

Density = $384.28+0.0057\times T^2-2.9901\times T$

Thermal conductivity = $0.0102+2\times10^{-07}\times T^2-3\times10^{-06}\times T$

For air

Dynamic viscosity= $3\times10^{-06}+4\times10^{-15}\times T^3-2\times10^{-11}\times T^2+5\times10^{-08}\times T$

Specific heat at constant pressure = $950.63+6\times10^{-08}\times T^3-0.0002\times T^2+0.2715\times T$

Density = $359.5\times T^{-1.0027}$

Thermal conductivity = $-(0.0006-0.0001\times T-1\times10^{-11}\times T^3+5\times10^{-08}\times T^2)$

3.5 Outlet Mean Temperature

To be able to calculate the overall performance of the heat exchanger, the mean temperature at the outlet of the heat exchanger is to be attained. The velocity weighted mean temperature across a boundary is defined as

$$T_0 = \frac{\int Tuds}{\int uds}$$

Where *ds* is the boundary length element.

3.6 Equations for Calculation of Heat Transfer Coefficient

Working fluids are passed through the gap between the plates of MEMS heat exchanger. The mode of heat transfer is convection and steady state condition is assumed. So heat transfer in fluid can be expressed as

$Q_{fluid} = \dot{m} C_p (T_0 - T_i)$

Where T_0 is outlet mean temperature.

Again, $Q_{fluid} = Q_{conv}$

$Q_{conv} = h A (T_w - T_m)$

Where, $T_m = (T_0 + T_i) / 2$

T_w = wall temperature which is assumed to be 363 K (90 °C). This value is chosen as the boiling point of water is 100 °C and other working fluids used in this analysis remain vapor in this temperature. If a value greater than 90 °C is chosen, then water starts changing its phase and bubbles may begin to form which is undesirable for this study.

The averaged heat transfer coefficient, h and the mean Nusselt number, Nu are estimated as follows:

$h = \dot{m} C_p (T_0 - T_i) / A (T_w - T_m)$

i.e., $h = \rho U_{av} A_1 C_p (T_0 - T_i) / A_2 (T_w - T_m)$

and $Nu = h D_h / k$

where D_h is the hydraulic diameter and D_h =(4 x Area)/Perimeter

Reynolds number is calculated as

$Re = \rho U_{av} D_h / \mu$

U_{av} is the mean velocity of fluid.

Prandtl number is calculated as

$Pr = C_p \mu / k$

3.7 Equations for Calculation of Effectiveness

The heat exchanger effectiveness is defined as

$$\text{Effectiveness, } \varepsilon = \frac{\text{Actual heat transfer}}{\text{Maximum possible heat transfer}}$$

To determine the maximum possible heat transfer for the heat exchanger, the maximum value needs to be recognized that could be attained if either of hot and cold fluids were to undergo a temperature change equal to the maximum temperature difference present in the exchanger, which is the difference in the entering temperatures for the hot and cold fluids. The fluid which might undergo this maximum temperature difference is one having the minimum value of $\dot{m} c$ because the energy balance requires that the energy received by one fluid be equal to that given up by other fluid; so, maximum possible heat transfer is expressed as

$$q_{\max} = (\dot{m}\, c)_{\min} (T_{h_{inlet}} - T_{h_{outlet}})$$

The minimum fluid may be either the hot or cold fluid, depending on the mass-flow rates and specific heats.

For a parallel flow heat exchanger where cold fluid is the minimum fluid, effectiveness can be expressed as

$$\varepsilon = \frac{\dot{m}_c\, c_c (T_{c_2} - T_{c_1})}{\dot{m}_c\, c_c (T_{h_1} - T_{c_1})}$$

i.e., $\varepsilon = \dfrac{(T_{c_2} - T_{c_1})}{(T_{h_1} - T_{c_1})}$

Where, T_{c_2} is outlet mean temperature, T_o

T_{c_1} = 321 K (48 °C) (assumed)

Besides water, three refrigerants were used as working fluid during this analysis. Among them, R113 shows the highest boiling point of 47.6 °C. R11 and ammonia remain at vapor phase whereas water is liquid at this temperature. So if the temperature range is chosen as 48°C to 90 °C, then all working fluids remain at single phase in this range. Thus it is possible to conduct this analysis for only single phase flow.

T_{h_1} = 363 K, assuming a hot fluid flows over the heated wall surface

The expression becomes

$$\varepsilon = \frac{T_0 - 321}{363 - 321}$$

i.e.,

$$\varepsilon = \frac{T_0 - 321}{42}$$

3.8 Grid Dependency Test

This analysis has been performed by solving Navier-Stokes equations and the convection and conduction equation by using a commercial finite element package FEMLAB 3.0. Before solving the problem, the geometry has been meshed with triangular elements. Maximum element size for global mesh parameters has been used as 7e-4 whereas for inlet and outlet boundaries the value has been maintained at 2e-5. It means the elements at the inlet and outlet boundaries are finer than those of other boundaries. Figure 3.4 shows MEMS heat exchanger in mesh mode. To investigate the influence of number of elements for base mesh on the simulation, several trails have been conducted.

Such as for pitch length of 0.95 mm and water as working fluid the following outlet mean temperatures have been found for different number of elements of base mesh

Table 3.2 Outlet mean temperature for different number of elements

Number of elements of base mesh	Outlet mean temperature (K)
8000	352.466
9000	354.67
9027	354.73
9050	354.73
9080	354.73

Assessments are conducted to obtain a fixed value of temperature. When the magnitude of outlet mean temperature becomes set for a value, the trail is stopped. The lowest value of the number of elements for this result has been considered as sufficient to correctly evaluate heat transfer parameters. For example, to correctly evaluate heat transfer data number of elements for pitch 0.95 mm has been found as 9027

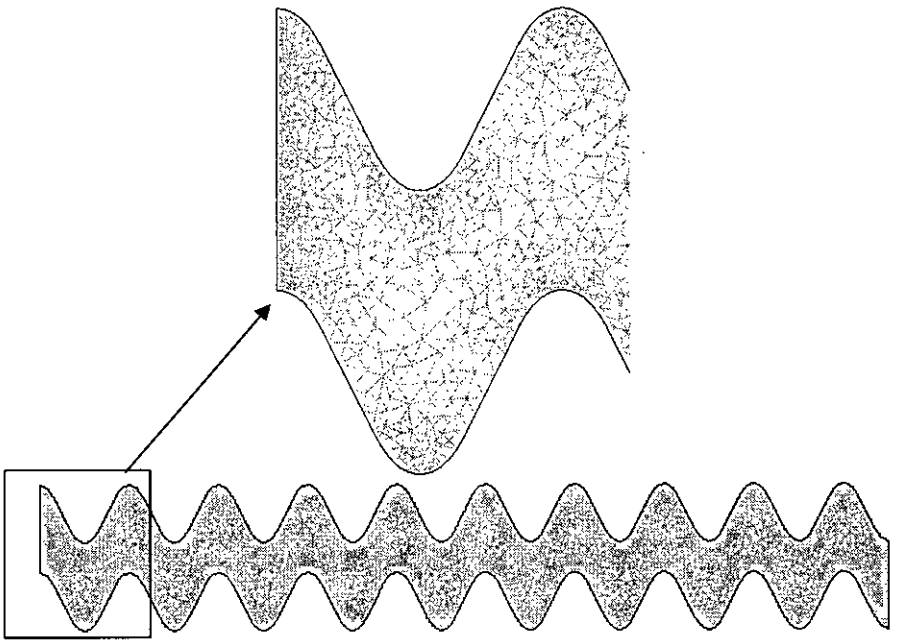

Figure 3.5 MEMS heat exchanger of pitch 0.95 mm in mesh mode

Similarly,

Number of elements for pitch 0.475 mm: 14051

Number of elements for pitch 0.2375 mm: 13476

Number of elements for pitch 0.11875 mm: 13013

Chapter 4

Results and Discussion

The overall performance of MEMS heat exchanger is evaluated by using a commercial finite element package [FEMLAB 3.0 described in Appendix B] in this present research. This investigation reveals the effect of flow of different type of fluids through the MEMS channels on heat transfer behaviour and thus may be a help to choose right working fluid under right conditions. For validation of present work, results obtained from the analysis are compared with previous results available in the literature. Temperature range has been chosen such as that the analysis can be accomplished for single phase flow. By increasing peaks of wavy surfaces, it is found that outlet mean temperature increases. The parameters which are used for constants and expressions during the analysis are shown in Table 4.1.

Table 4.1: Parameters used during analysis as Input data

Parameters	Symbol	Unit
Inlet Temperature	T_i	K
Wall Temperature	T_h	K
Average velocity	U_{av}	m/s
Density	ρ	kg/m^3
Thermal conductivity	k	W/m.K
Dynamic viscosity	μ	kg/m.s
Specific heat at constant pressure	C_p	J/kg.K

4.1 Validation of the Analysis

For numerical validation, air has been used as a working fluid and flowed through the gap between the plates. The mode of heat transfer in air is convection and a steady state condition is assumed. The geometry has been a wavy surface of pitch 0.95 mm and the velocity of air has been varied to obtain a desirable range of values for Reynolds number. The aim has been to maintain laminar region in the flow field. The section of the heat exchanger which is considered in the present analysis can be compared with a duct. In a duct, the Reynolds number is used as a criterion for laminar and turbulent flow. For $Re = \rho U_{av} D_h / \mu > 2300$ the flow is usually observed to be turbulent. In this study, different outlet mean temperature of air has been attained for several Reynolds number from 52 to 225.16. Heat transfer coefficient and Nusselt numbers have been calculated using the expressions discussed in the previous chapter. These values of Nusselt number is plotted against Reynolds number for comparison with other results available in the literature. It has been seen that for a low value of Reynolds number the increase in Nusselt number is sharp, after that it starts increasing slowly with the increase in Reynolds number.

Similar type of analysis was done by Hardt *et al.*[2] who showed that the sine-shaped walls affect the flow pattern in such a way that a substantial heat transfer enhancement was achieved, reflected in Nusselt numbers of up to 32. They showed the variation of Nu with Re where in case of doubt (i.e., a weak dependence of *Nu* on position) the Nusselt number was evaluated close to the channel outlet. Another analysis done by Hossain *et al.*[4] showed that Nusselt number increases with the increase in Re. Steady flow gives modest increase in Nusselt number but unsteady flow gives rapid increase due to better mixing of core and near the wall fluids, but this rate of increase again slows down as Re is increased more.

Both these results obtained from the previous work along with the results of present study are plotted in the same graph on Figure 4.1. Good agreement is found with the results of Hossain *et al.* whereas a slight deviation is seen while comparing with the result of Hardt *et al.* The qualitative agreement of the results implies the validity of the present

simulation. Table 4.2 shows the comparison of the results of the present analysis with the results available in the previous work.

Table 4.2: Comparison of the results of the Present model with the results of earlier research works

Present Model		**Model of Hossain *et al***		**Model of Hardt *et al***	
Re	**Nu**	**Re**	**Nu**	**Re**	**Nu**
52.49	6	100	10	30	7
107.8	9	200	12.5	50	9
165.66	11	300	13.5	90	11.5
225.16	12	400	14	140	13
				200	14.5
				300	16
				400	17

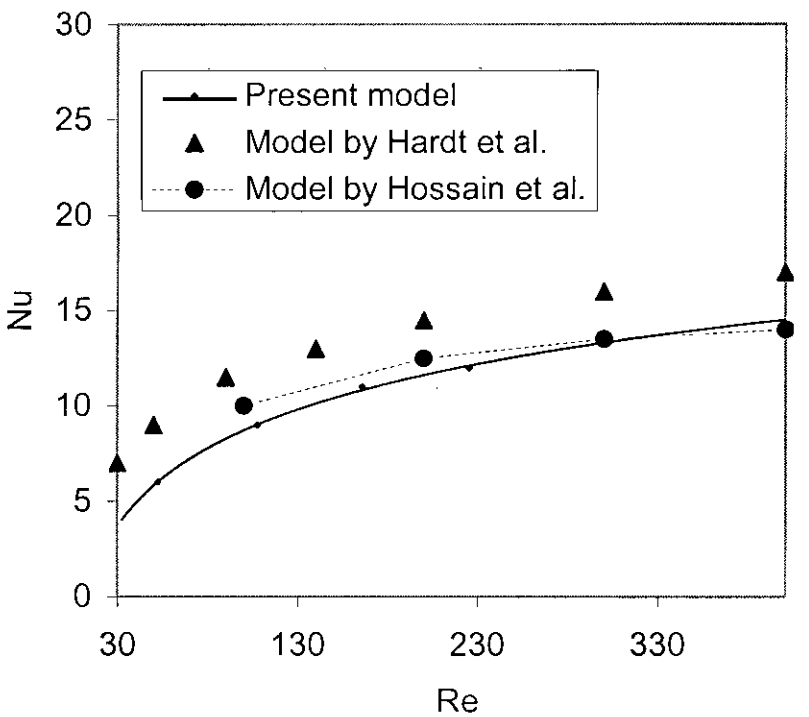

Figure 4.1 Variation of Nusselt number (Nu) with different Reynolds number (Re) for the pitch = 0.95 mm and air as working fluid and comparison of the result of the present model with the results [2, 4] available in the literature.

4.2 Effect of Different Parameters with Reynolds Number

The objective of this analysis is to evaluate the performance of heat exchanger using different working fluids, careful consideration has been given to the fact that fluid transport properties, viscosity, thermal conductivity and density may vary considerably with temperature. Such property variations distort both velocity and temperature profiles, so all fluid properties are evaluated at the mean fluid temperature. The physical mechanism of viscosity is one of momentum exchange. As laminar flow has been considered here, molecules may move from one lamina to another, carrying with them a momentum corresponding to the velocity of the flow. There is a net momentum transport from regions of high velocity to regions of low velocity, thus creating a force in the direction of the flow. The rate at which momentum transfer takes place is dependent on the rate at which the molecules move across the fluid layers. In a gas, molecules would move about with some average speed proportional to the square root of the absolute temperature since, in the kinetic theory of gases, temperature is identified with the mean kinetic energy of a molecule. The faster the molecules move the more momentum they transport so air is used as working fluid in most of the research works. In this case, performance of other fluids must be investigated so that their performance can be compared with air.

Figure 4.2 and 4.3 show the variation of effectiveness and Nusselt number with Reynolds number. The figures also indicate the optimum conditions for different working fluids. These figures show for an optimum value of Re = 88, both the effectiveness and Nusselt number of water are high. Similarly optimum values of Reynolds number for air, ammonia, Freon 11 and Freon 113 are found to be around 205, 160, 280 and 280 respectively. The optimum points for water, air, ammonia, Freon 11 and Freon 113 are denoted as A, B, C, D and E respectively in figures 4.2 and 4.3. These are optimum values of these fluids when used in a MEMS heat exchanger of wavy surface and pitch 0.95 mm. For optimum value of Reynolds number of 280, Freon 11 exhibits the greatest effectiveness, which is 79%. For Freon 113, ammonia, water and air the value of effectiveness for optimum Reynolds number are 72%, 77%, 67% and 64% respectively.

It is evident from the figure that with increase in Reynolds number, Nusselt number also increases but effectiveness decreases. It means although the flow rate is increased the effectiveness does not increase. It may happen due to the fact the heat exchanger is more effective at lower flow rate [13]. Figures 4.4 to 4.8 show the variation of Nusselt number with the product of Reynolds number and Prandtl number which indicates the linear relationship between Nusselt number and the product of Reynolds number and Prandtl number. It is found that in case of water and ammonia there are straight line relationship between Nusselt number and the product of Reynolds number and Prandtl number. But for air, Freon-11 and Freon-113 rate of increasing of Nusselt number diminishes after a certain point with increase in the product of Reynolds number and Prandtl number.

Figure 4.9 shows the decrease in outlet mean temperature with increase in Reynolds number. As fluid velocity is increased, it does not get enough time to absorb heat from its surroundings; as a result, outlet mean temperature does not increase as expected. The outlet mean temperature is needed to calculate effectiveness. The expression has been shown in the previous chapter.

There is no denying the fact that the use of the wavy-surfaced wall cause increase in heat transfer area. Therefore, more heat flows to the coolant. Furthermore, the recirculation / reverse flow enhances the fluctuations of fluid molecule which lead to even better convection heat transfer. Thus for a wavy surfaced heat exchanger, the Nusselt number increases with the increase in Reynolds number. Figures 4.10 and 4.11 show the variation of heat transfer coefficient with Reynolds number for different working fluids. It is apparent from the figures that water shows the highest value of heat transfer coefficient among the fluids. In case of water, heat transfer coefficient increases sharply with increase in Reynolds number whereas for other fluids it increases slowly with Reynolds number.

Reynolds number is varied by varying velocity of the fluid. Reynolds number depends on fluid properties such as density, dynamic viscosity, hydraulic diameter and fluid velocity. Table 4.3 shows the variation of outlet mean temperature, effectiveness, heat transfer

coefficient Nusselt number and Prandtl number calculated from the expressions discussed in the previous chapter for each fluid obtained for different Reynolds number.

Table 4.3: Variation of Different Parameters with Reynolds number for Different Fluids in wavy surface MEMS heat exchanger

Fluid: air , pitch :0.95 mm					
Reynolds number	Outlet Temperature	Effectiveness	Heat Transfer Coefficient	Nusselt Number	Prandtl Number
52.49	361.54	96.604	89.298	5.477	0.648
107.8	355.96	83.627	139.36	8.659	0.649
165.66	350.95	71.976	165.79	10.45	0.6497
225.16	347.12	63.069	182.96	11.61	0.65

Fluid: water, pitch: 0.95 mm					
Reynolds number	Outlet Temperature	Effectiveness	Heat Transfer Coefficient	Nusselt Number	Prandtl Number
134.09	345.967	60.388	5048.88	13.71	2.48
174.736	342.4	52.093	5489.36	14.97	2.55
209.62	339.84	46.139	5857.49	16.05	2.68
245.34	337.9	41.627	6158.05	16.93	2.76

Fluid: ammonia, pitch: 0.95 mm					
Reynolds number	Outlet Temperature	Effectiveness	Heat Transfer Coefficient	Nusselt Number	Prandtl Number
135.44	355.575	82.732	249.04	13.96	1.44
188.55	352.18	74.837	289.17	15.43	1.437
237.22	349.575	68.779	314.2	16.92	1.429
282.48	347.49	63.930	331.39	18.002	1.425

Fluid: Freon11, pitch: 0.95 mm					
Reynolds number	Outlet Temperature	Effectiveness	Heat Transfer Coefficient	Nusselt Number	Prandtl Number
86.78	361.73	97.046	32.395	7.04	0.905
207.45	356.35	84.534	58.89	12.81	0.886
289.49	353.03	76.813	69.114	15.03	0.875
433.24	348.37	65.976	80.186	17.488	0.8589

Fluid: Freon113, pitch: 0.95 mm					
Reynolds number	Outlet Temperature	Effectiveness	Heat Transfer Coefficient	Nusselt Number	Prandtl Number
90.69	360.93	95.186	31.296	7.26	0.926
219.07	353.325	77.5	52.47	12.17	0.923
310.44	349.016	67.479	59.66	13.84	0.9197
480.04	343.4	54.418	67.37	15.63	0.9148

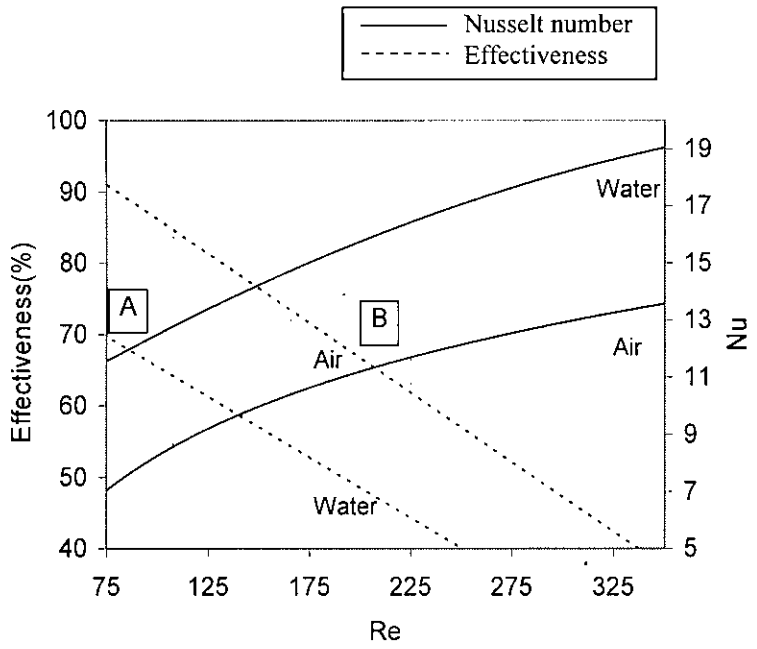

Figure 4.2 Variation of effectiveness and Nusselt number with Reynolds number of wavy surface of MEMS heat exchanger for air and water for pitch = 0.95 mm

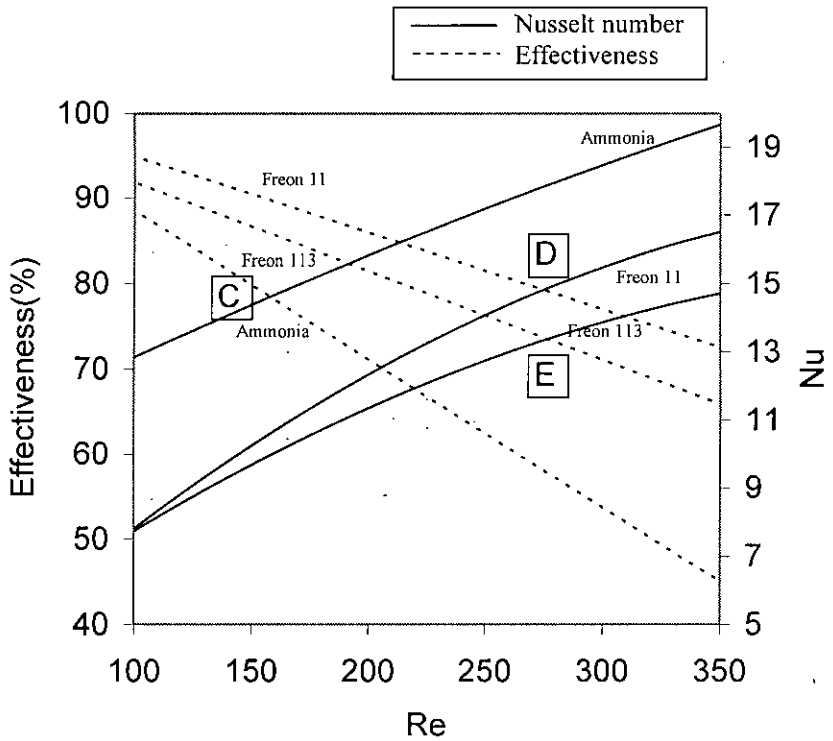

Figure 4.3 Variation of effectiveness and Nusselt number with Reynolds number of wavy surface of MEMS heat exchanger for different working fluids for pitch = 0.95 mm

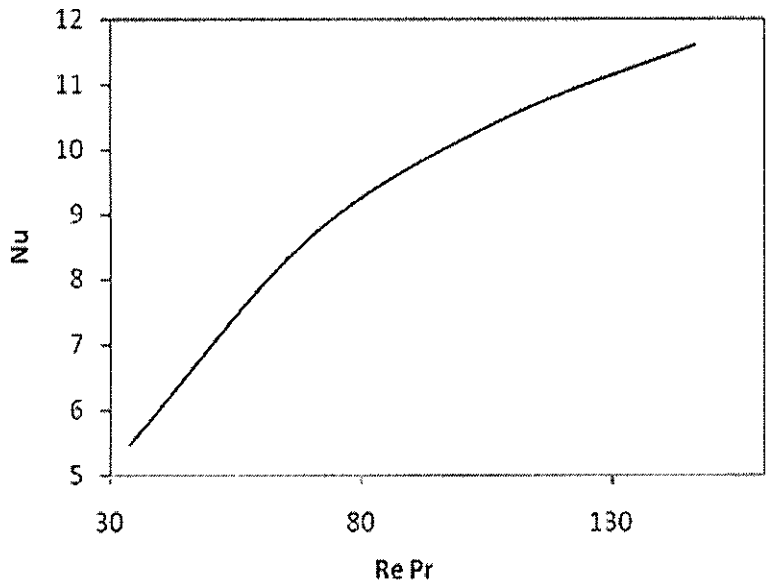

Figure 4.4 Variation of Nusselt number with the products of Reynolds number and Prandtl number of wavy surface of MEMS heat exchanger for air and for pitch = 0.95 mm

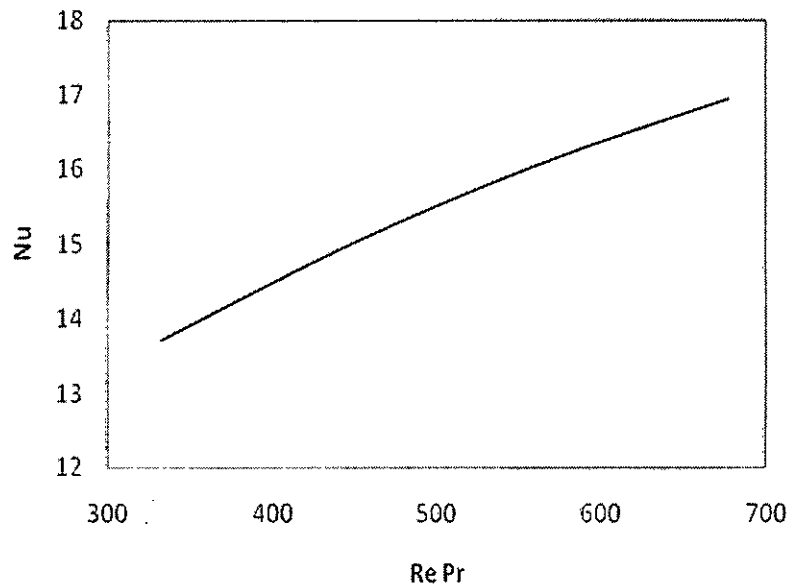

Figure 4.5 Variation of Nusselt number with the products of Reynolds number and Prandtl number of wavy surface of MEMS heat exchanger for water and for pitch = 0.95 mm

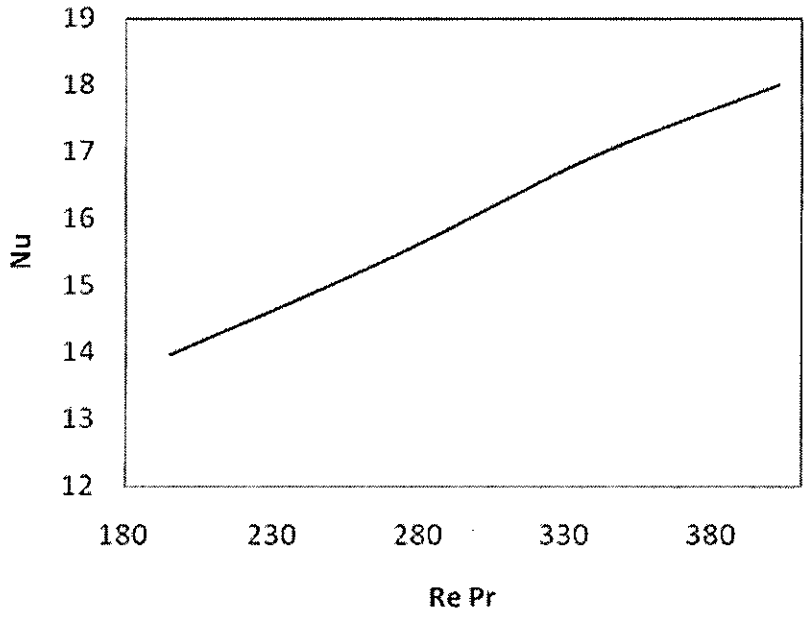

Figure 4.6 Variation of Nusselt number with the products of Reynolds number and Prandtl number of wavy surface of MEMS heat exchanger for ammonia and for pitch = 0.95 mm

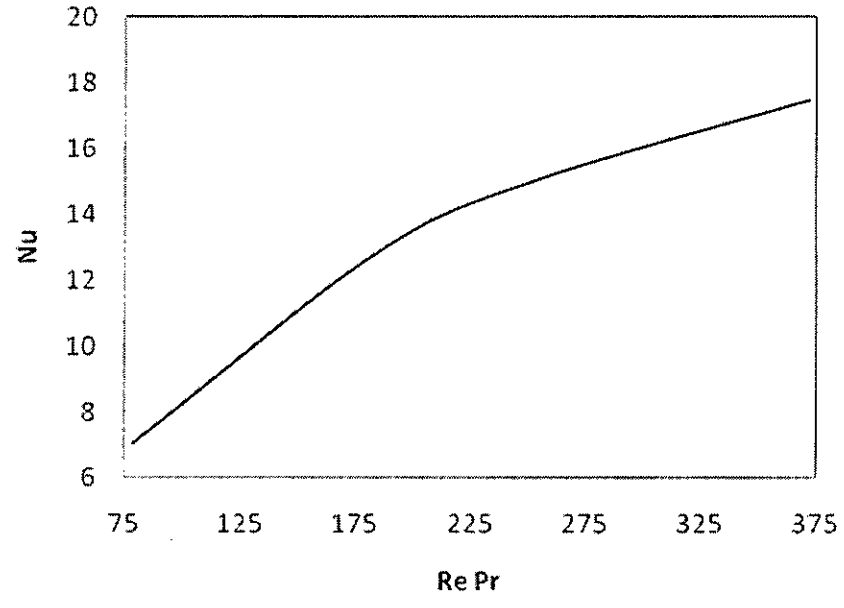

Figure 4.7 Variation of Nusselt number with the products of Reynolds number and Prandtl number of wavy surface of MEMS heat exchanger for Freon 11 and for pitch = 0.95 mm

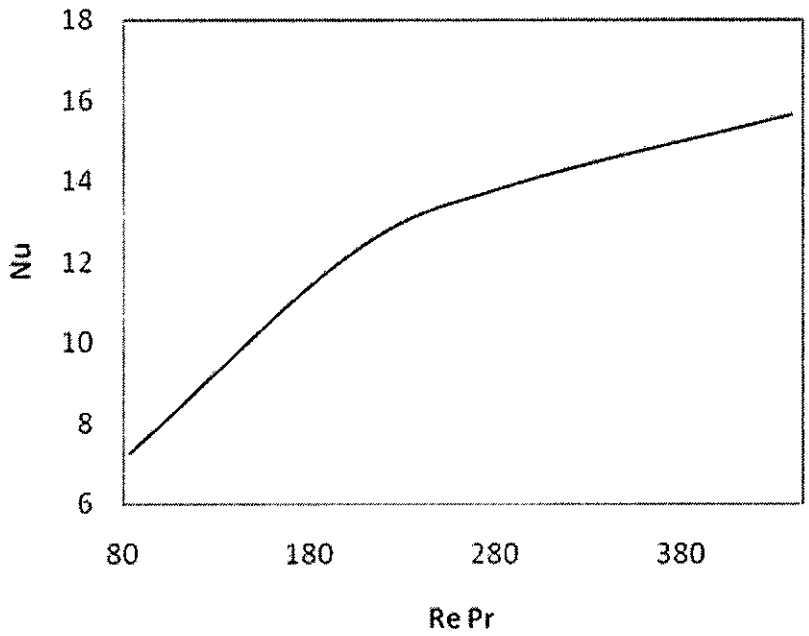

Figure 4.8 Variation of Nusselt number with the products of Reynolds number and Prandtl number of wavy surface of MEMS heat exchanger for Freon 113 and for pitch = 0.95 mm

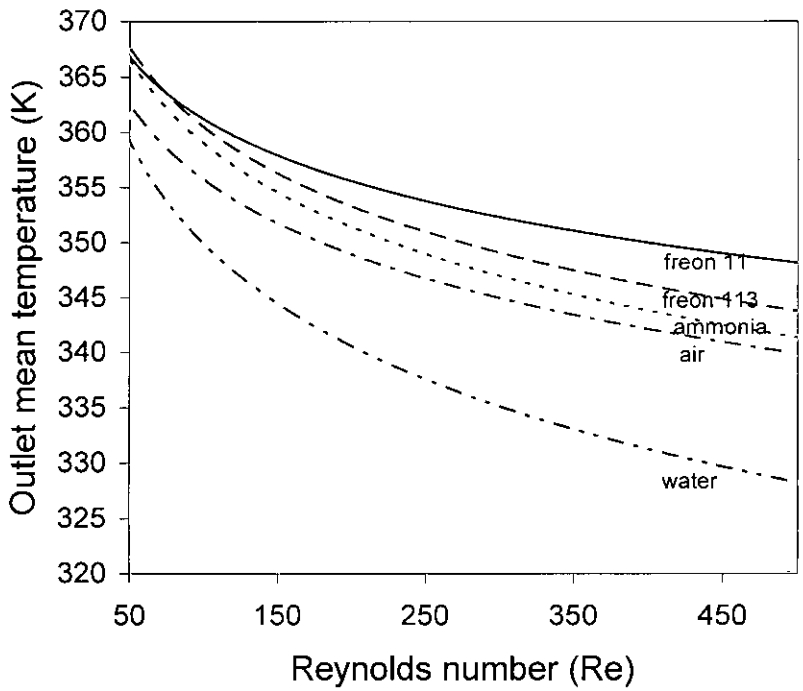

Figure 4.9 Variation of outlet mean temperature with Reynolds number of wavy surface of MEMS heat exchanger for various working fluids for pitch = 0.95 mm

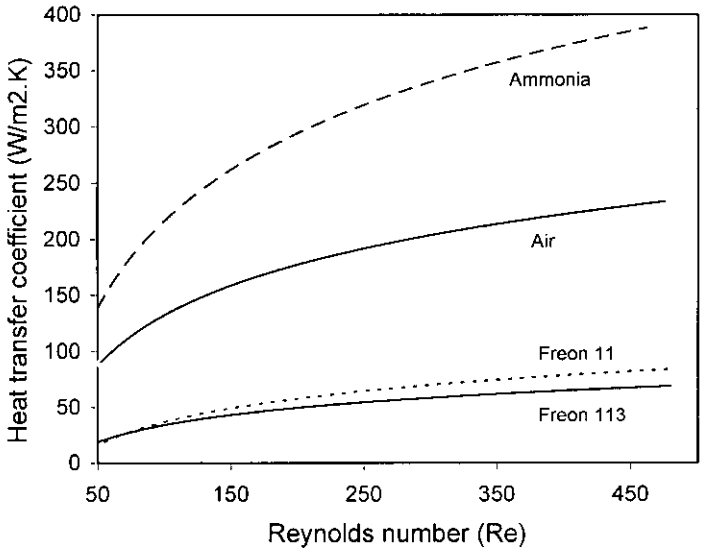

Figure 4.10 Variation of heat transfer coefficient with Reynolds number of wavy surface of MEMS heat exchanger for various working fluids for pitch = 0.95 mm

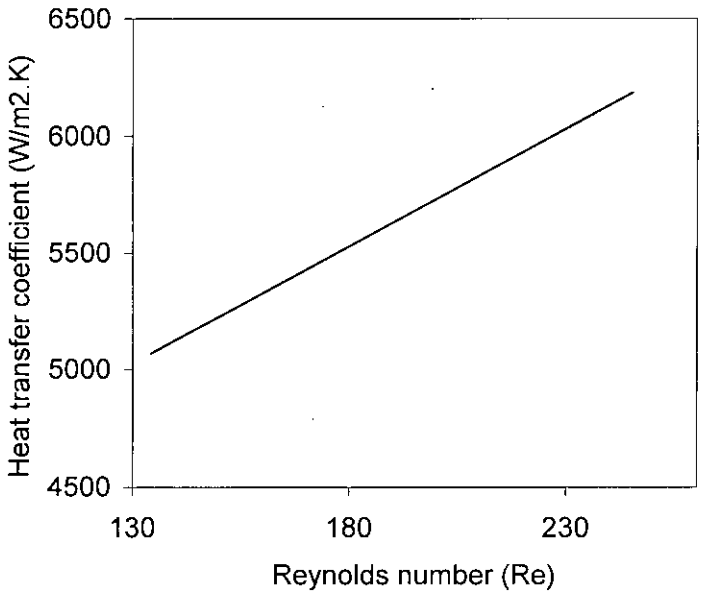

Figure 4.11 Variation of heat transfer coefficient with Reynolds number of wavy surface of MEMS heat exchanger for water for pitch = 0.95 mm

4.3 Effect of Different Parameters with Pitch

The working fluids are passed through the MEMS heat exchanger with different pitches to evaluate their performance. The number of peaks in wavy surface is increased in such a way that total length of a plate remains same. As a result, distance between two peaks i.e., pitch is reduced from a value of 0.95 to 0.11875 mm. For all cases, average velocity has been maintained at 0.015 m/s. Figure 4.12 depicts the variation of outlet mean temperature with different pitches. It is seen from Figure 4.12 that as the pitch increases the outlet mean temperature decreases. It means as the number of peaks is increased in the wavy surface, the surface area also increases which plays an important role to enhance heat transfer from the wall surface to the fluid. As a result, the fluid in a heat exchanger with more peaks can remove more heat than that by the heat exchanger of the same length and amplitude with less number of peaks. Consequently, the mean temperature at the outlet gets higher in case of low pitch (more no. of peaks) heat exchanger. It is also an indication of better performance for a heat exchanger.

The boiling point of R-11 at atmospheric pressure is 23.77°C which exhibits the highest outlet mean temperature when used as a coolant in a MEMS heat exchanger. The temperature range used in the analysis is 48°C to 90°C. In this range, only water remains liquid (boiling point 100°C), boiling point of R-113 and ammonia is 47.6°C and -33.3°C respectively at atmospheric pressure [14].

Another conspicuous point of this figure is water shows lowest outlet mean temperature in comparison to other fluids which remain vapour in this particular temperature range. The reason may be for the greater values of enthalpy and entropy of saturated vapours whereas water as a liquid has low enthalpy as well as entropy. Figures 4.13 to 4.17 show temperature distribution for different surfaces of MEMS heat exchanger when water is working fluid and pitch length is 0.95 mm. From the figures it is seen that low temperature region decreases as surface area increases from plain surface to wavy surface and pitch length decreases from 0.95 to 0.11875 mm. It happens like this because as heat transfer area is increased in case of plain surface to form wavy surface or peaks are

increased in wavy surface then fluid can absorb more heat than before and becomes hot comparatively at earlier stage.

As effectiveness is related to temperature, it shows the same pattern of curve as temperature [Figure 4.18]. Figure 4.19 shows Reynolds number variation with pitch which remains almost constant for all cases. Figure 4.20 to 4.23 shows that the heat transfer (calculated in Watt) increases gradually with the increase in pitch. These figures also show that the value of heat transfer in wavy surface is greater than that of plain surface which is the consequence of enhancement of heat transfer in wavy surface. Highest value of heat transfer of water sets itself as the most effective coolant. In spite of having lowest outlet mean temperature, water can transfer heat in a more convenient way because its heat transfer coefficient is much higher than other fluids. Heat transfer coefficient is related to other parameters such as temperature dependent properties of water, velocity and heat transfer area. Velocity and area being the same for all fluids, refrigerants which have lower heat transfer coefficient, show lower values of heat transfer. For changing the pitch length from 0.95 mm to 0.11875 mm, water shows the highest value of increment of heat transfer which is 13.27 %, ammonia, Freon 113, Freon 11 shows increment of 5.4%, 5.7% and 4.5% respectively. Tables 4.4 and 4.5 show the values of different parameters for MEMS heat exchanger with wavy surface and plain surface.

Table 4.4: Variation of Different Parameters with pitch for Different Fluids in wavy surface MEMS heat exchanger

For wavy surface and fluid: water				
Pitch (mm)	Temperature (K)	Effectiveness (%)	Reynolds number	Heat Transfer (Watt)
0.95	354.73	80.76	75.414	20.139
0.475	356.93	85.88	77.16	21.408
0.2375	358.467	89.46	78.35	22.314
0.11875	359.467	91.78	79.15	22.812

For wavy surface and fluid: ammonia				
Pitch (mm)	Temperature (K)	Effectiveness (%)	Reynolds number	Heat Transfer (Watt)
0.95	361.467	96.43	56.75	0.6354
0.475	362.067	97.83	57.38	0.6543
0.2375	362.4	98.6	57.73	0.6656
0.11875	362.6	99.06	57.94	0.6698

For wavy surface and fluid: Freon 11				
Pitch (mm)	Temperature (K)	Effectiveness (%)	Reynolds number	Heat Transfer (Watt)
0.95	361.73	97	86.78	0.143
0.475	362.2	98.139	87.585	0.1464
0.2375	362.53	98.9	88.149	0.1488
0.11875	362.67	99.23	88.388	0.1494

For wavy surface and fluid: Freon 113				
Pitch (mm)	Temperature (K)	Effectiveness (%)	Reynolds number	Heat Transfer (Watt)
0.95	360.93	95.18	90.69	0.1407
0.475	361.73	97.046	91.63	0.1451
0.2375	362.2	98.139	92.183	0.1477
0.11875	362.46	98.74	92.49	0.1487

Table 4.5: Variation of Different Parameters for Different Fluids in plain surface MEMS heat exchanger

For plain surface and different fluids				
Fluid	Temperature (K)	Effectiveness (%)	Reynolds number	Heat Transfer (Watt)
ammonia	357.13	86.34	52.24	0.5094
Freon 11	357.73	87.74	80.06	0.1173
Freon 113	357	86.05	86.193	0.1204
water	351.067	72.25	72.18	18.008

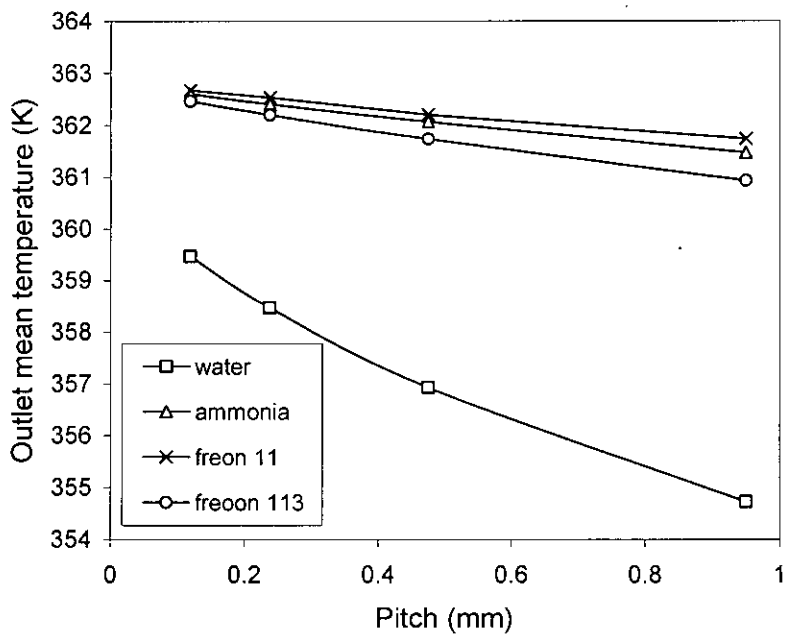

Figure 4.12 Variation of outlet mean temperature with different pitches of wavy surface of MEMS heat exchanger for various working fluids (U_{av} = 0.015 m/s)

Temperature distribution of different wavy surfaces of MEMS heat exchanger are shown below:

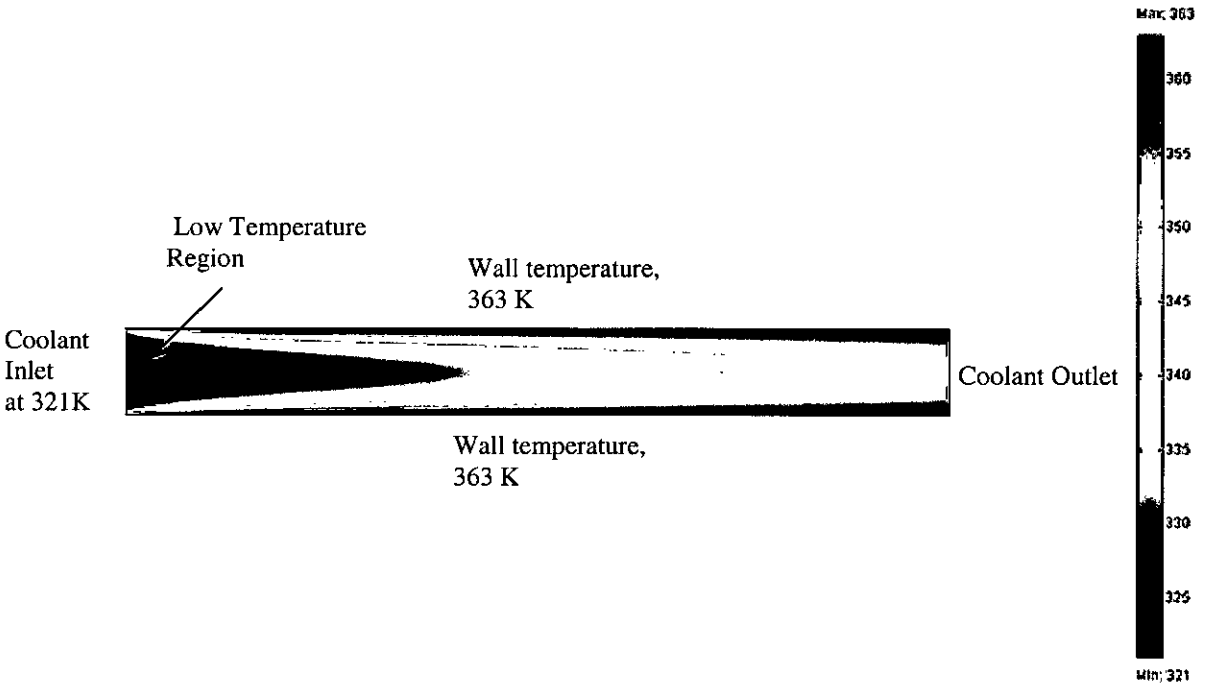

Figure 4.13: Temperature distribution in Plain Surface MEMS heat exchanger for water

Figure 4.14: Temperature distribution in Wavy Surface MEMS heat exchanger for pitch 0.95mm for water

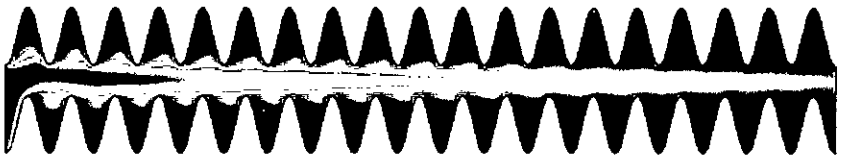

Figure 4.15: Temperature distribution in Wavy Surface MEMS heat exchanger for pitch 0.475 mm for water

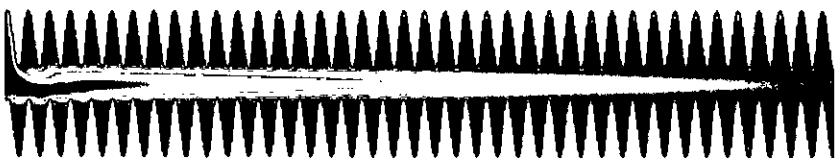

Figure 4.16: Temperature distribution in Wavy Surface MEMS heat exchanger for pitch 0.2375 mm for water

Figure 4.17: Temperature distribution in Wavy Surface MEMS heat exchanger for pitch 0.11875 mm for water

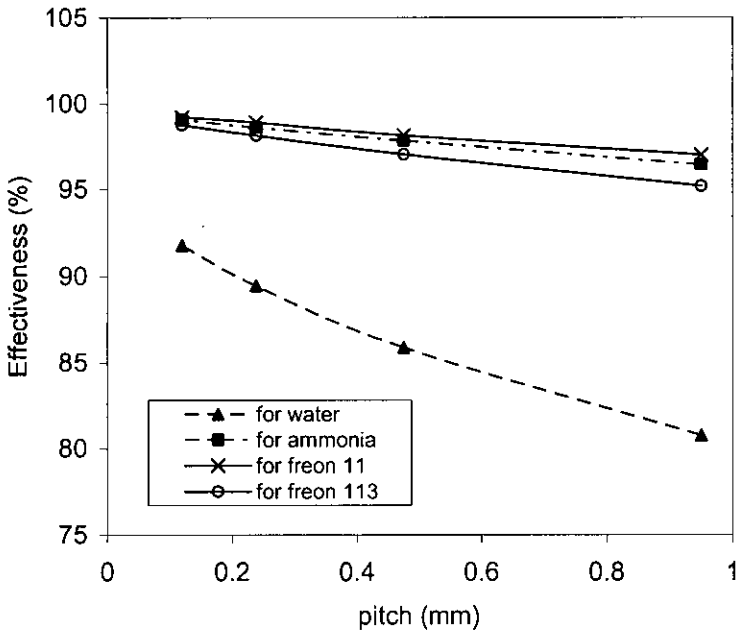

Figure 4.18 Variation of Effectiveness with different pitches of wavy surface of MEMS heat exchanger for various working fluids (U_{av} = 0.015 m/s)

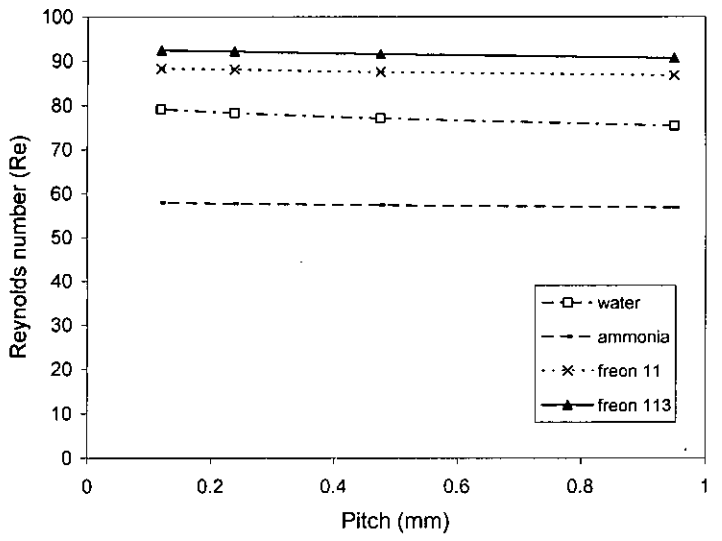

Figure 4.19 Variation of Reynolds number with different pitches of wavy surface of MEMS heat exchanger for various working fluids (U_{av} = 0.015 m/s)

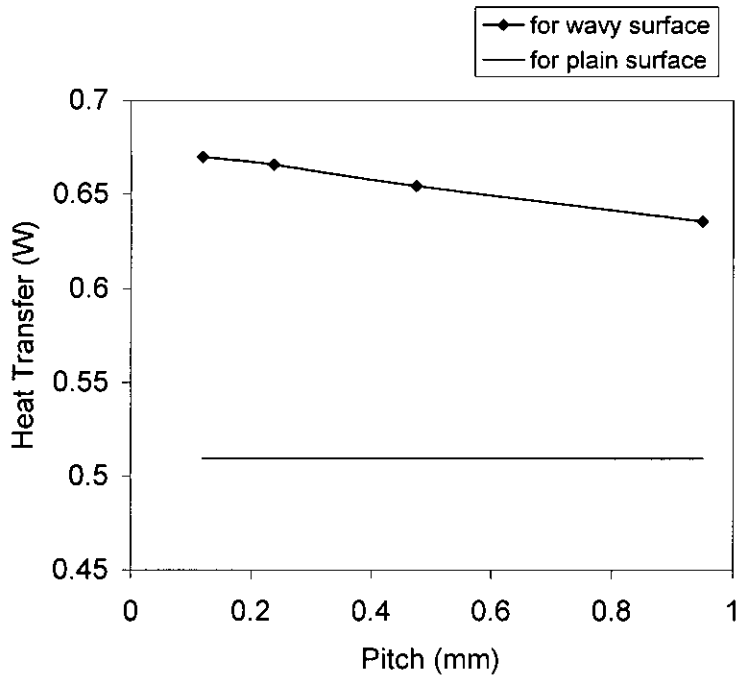

Figure 4.20 Comparison of heat transfer of ammonia between wavy surface and plain surface MEMS heat exchanger for U_{av} = 0.015 m/s

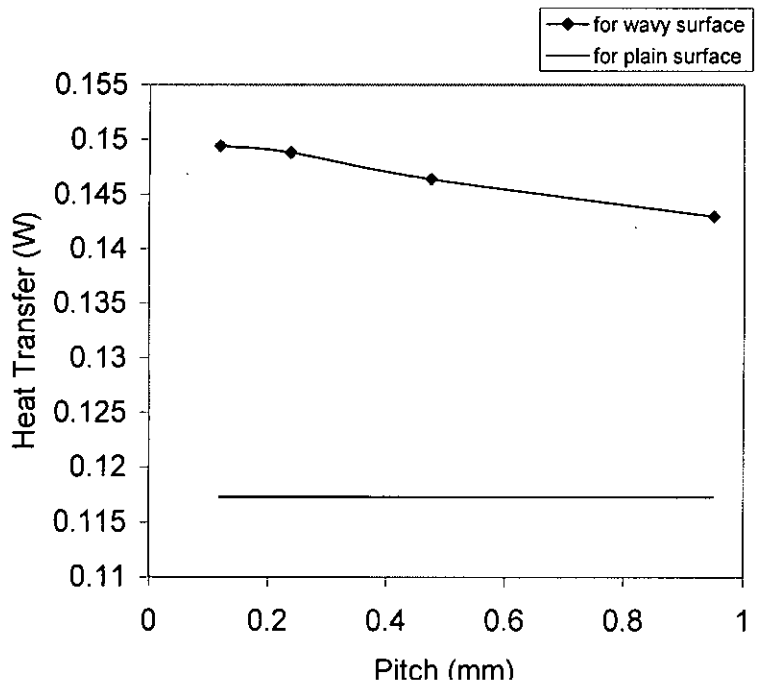

Figure 4.21 Comparison of heat transfer of Freon 11 between wavy surface and plain surface MEMS heat exchanger for U_{av} = 0.015 m/s

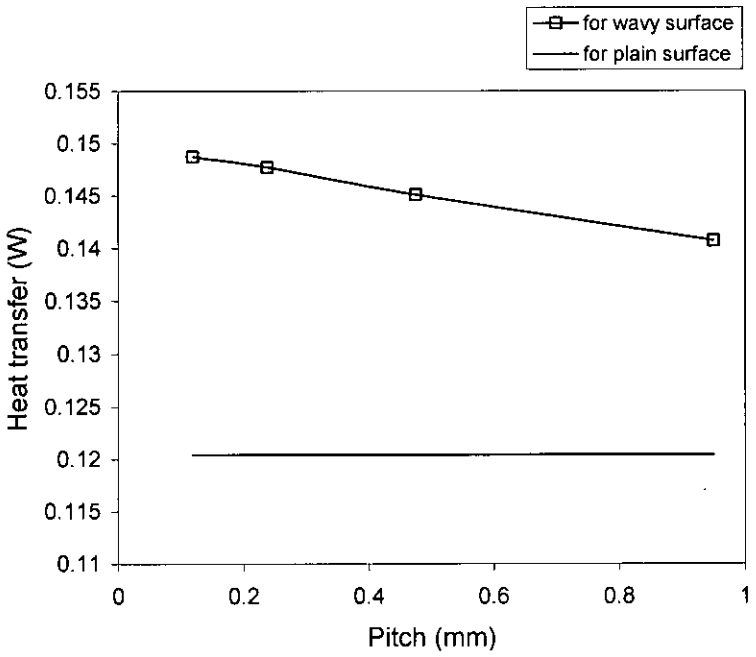

Figure 4.22 Comparison of heat transfer of Freon 113 between wavy surface and plain surface MEMS heat exchanger for U_{av} = 0.015 m/s

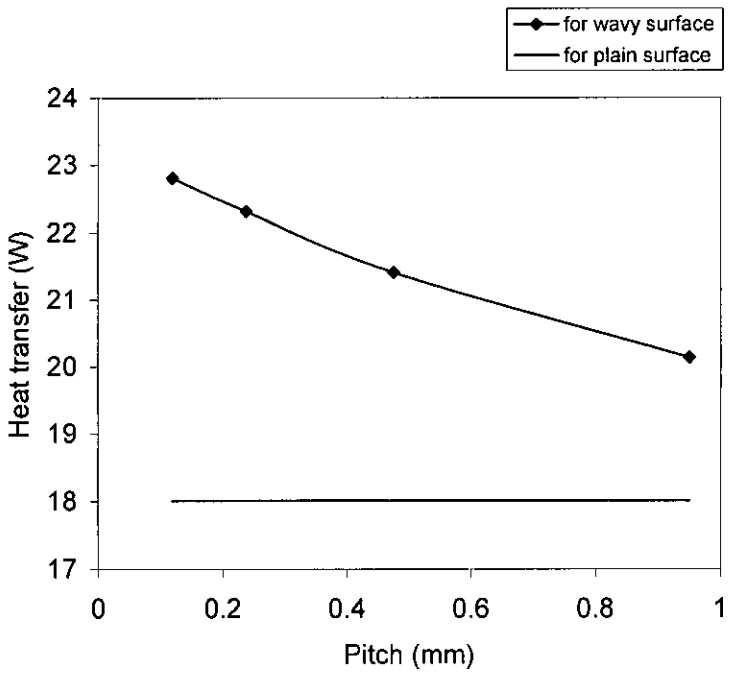

Figure 4.23 Comparison of heat transfer of water between wavy surface and plain surface MEMS heat exchanger for U_{av} = 0.015 m/s

4.4 Comparison of Effectiveness for Wavy and Plain Surface

Figures from 4.24 to 4.27 show comparison of effectiveness for wavy and plain surface for different fluids. It shows that as heat transfer area is larger for wavy wall in comparison to plain wall therefore heat transfer in fluid as well as outlet mean temperatures are greater in value for wavy surface which results in higher effectiveness. Among the fluids Freon 11 shows the highest effectiveness which is 99.23% whereas ammonia exhibits 99.06% effectiveness. These data reveal that refrigerants can also be used in MEMS heat exchanger as a coolant as these can remove heat from the heated wall in a more effective way.

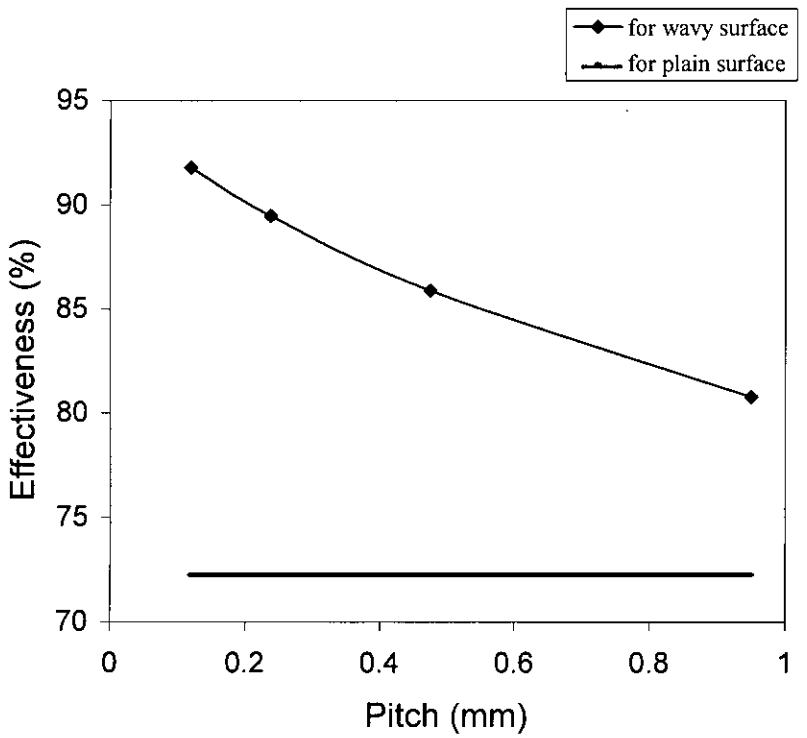

Figure 4.24 Comparison of effectiveness between wavy surface and plain surface MEMS heat exchanger for water

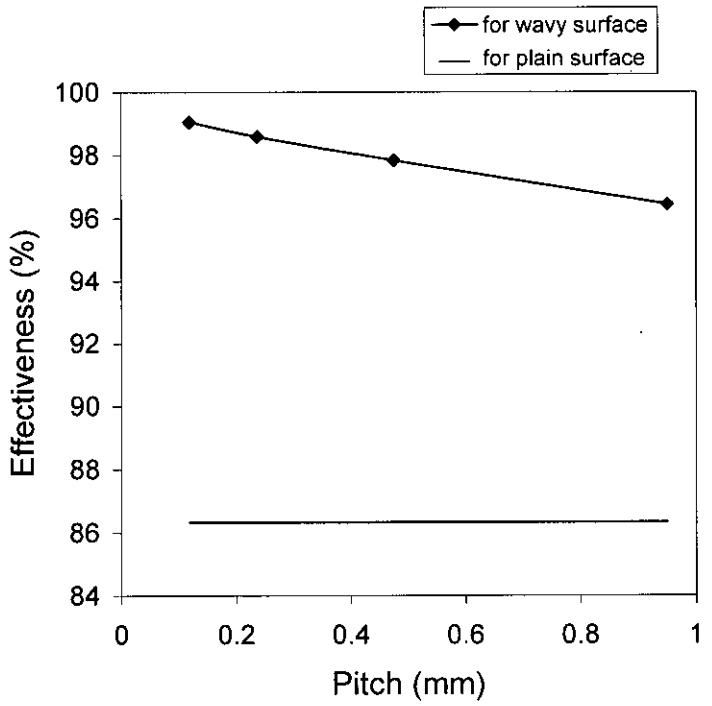

Figure 4.25 Comparison of effectiveness between wavy surface and plain surface MEMS heat exchanger for ammonia

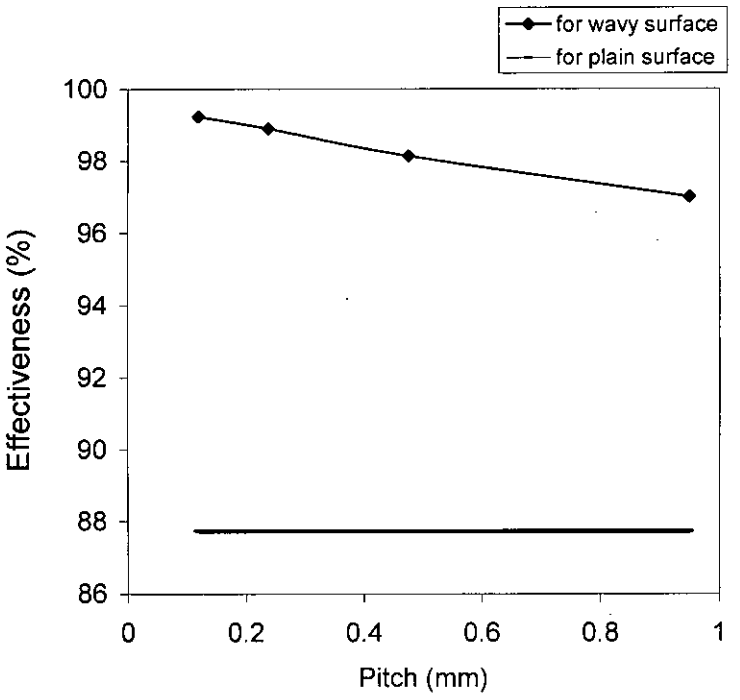

Figure 4.26 Comparison of effectiveness between wavy surface and plain surface MEMS heat exchanger for Freon 11

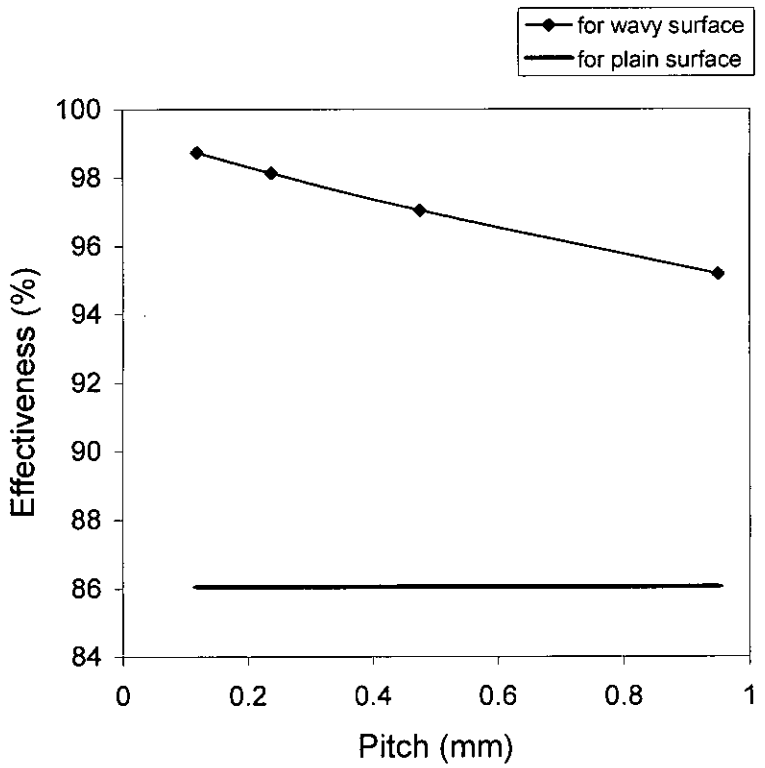

Figure 4.27 Comparison of effectiveness between wavy surface and plain surface MEMS heat exchanger for Freon 113

4.5 Flow Pattern of Different Working Fluids for Wavy Surface

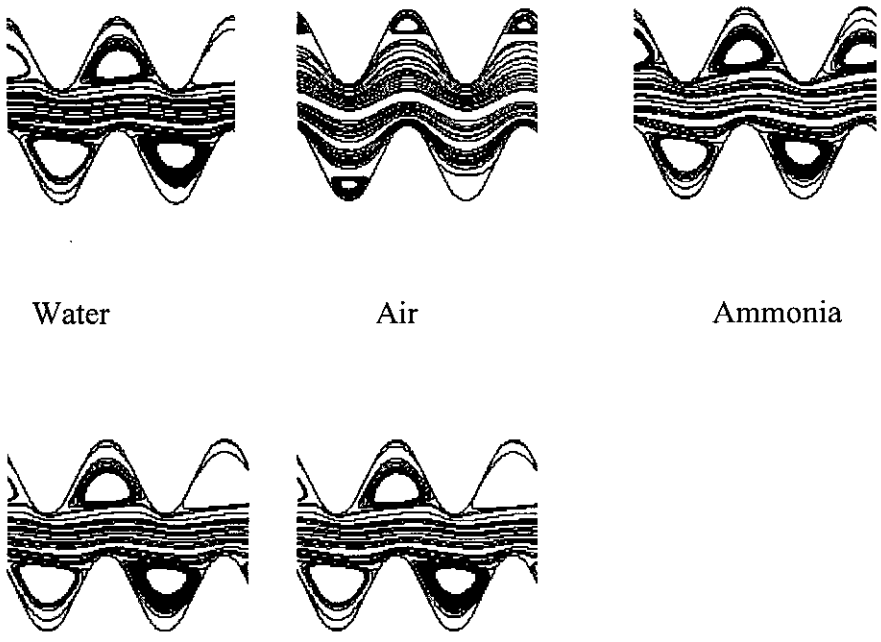

Figure 4.28 Pattern of velocity field in the clearance between the mating surfaces in the wavy surface MEMS heat exchanger of pitch length 0.95 mm

Water

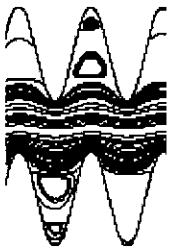

Air

Ammonia

Freon 11

Freon 113

Figure 4.29 Pattern of velocity field in the clearance between the mating surfaces in the wavy surface MEMS heat exchanger of pitch length 0.475 mm

Water

Air

Ammonia

Freon 11

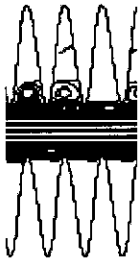

Freon 113

Figure 4.30 Pattern of velocity field in the clearance between the mating surfaces in the wavy surface MEMS heat exchanger of pitch length 0.2375 mm

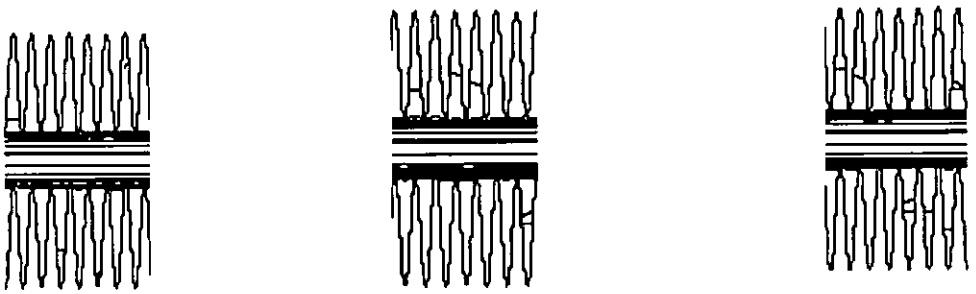

Water Air Ammonia

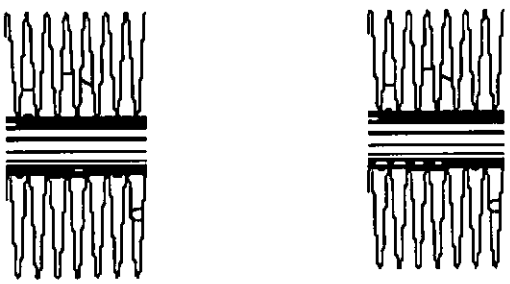

Freon 11 Freon 113

Figure 4.31 Pattern of velocity field in the clearance between the mating surfaces in the wavy surface MEMS heat exchanger of pitch length 0.11875 mm

The flow field inside the wavy enclosure is presented in terms of streamlines in Figures 4.28 to 4.31. The figure also shows the difference of flow structure at steady state for different fluids. It is apparent that the streamlines do not vary from one instant to the next as velocity at each point in the flow field remains constant with time i.e., steady flow is considered. The morphology of the stream function shows an ascending flow at each summit and a descending flow at each hollow of the sinusoidal profile. It is also seen that vortices are formed close to the convex sections of the wavy walls which is apparent for pitch length of 0.95 mm and 0.475 mm. Even for smaller offsets between the two boundary walls the fluid is driven to a path with small curvature. This effect is due to the convective term in the Navier-Stokes equation, which accounts for inertial forces on a moving fluid element and becomes important for high Reynolds numbers. The vortices tend to be diminished as the pitch length is reduced from 0.475 mm to 0.11875 mm.

4.6 Effect of Geometry on Effectiveness

The effectiveness and heat transfer of fluids vary with geometry which is shown in Figures from 4.32 to 4.39. In case of triangular surface MEMS heat exchanger when pitch is reduced from 0.475 to 0.11875 mm, the value of heat transfer does not vary much for most of the fluids while in case of rectangular surface heat exchanger, both the values of heat transfer and effectiveness remain same while pitch is reduced from 0.475 mm to 0.11875 mm. It means that increasing the peaks has no effect on effectiveness and heat transfer behaviour in case of triangular and rectangular surface. It is seen that rectangular surface shows the highest value of effectiveness while compared to that of other geometry. In case of less number of peaks the diminishing rate of the value of heat transfer and effectiveness is steeper in case of triangular surface than those of rectangular surface. For less number of peaks wavy surface shows good performance in heat transfer and effectiveness than triangular surface. From this aspect, it can be concluded that rectangular surface can be considered instead of wavy surface while designing MEMS heat exchanger as it is also easy to manufacture. Table 4.6 shows outlet mean temperature and effectiveness for triangular surface and rectangular surface MEMS heat exchanger.

Table 4.6: Outlet mean temperature and effectiveness for triangular surface and rectangular surface MEMS heat exchanger

For triangle surface and fluid: water		
Pitch (mm)	Outlet Temperature (K)	Effectiveness (%)
0.95	354.2	79.04
0.475	362.6	99.05
0.2375	362.8	99.5
0.11875	363	100

For rectangle surface and fluid: water		
Pitch (mm)	Outlet Temperature (K)	Effectiveness (%)
0.95	356.53	84.6
0.475	362.86	99.66
0.2375	362.86	99.66
0.11875	362.86	99.66

For triangle surface and fluid: ammonia		
Pitch (mm)	Outlet Temperature (K)	Effectiveness (%)
0.95	361.067	95.39
0.475	362.93	99.83
0.2375	363	100
0.11875	363	100

For rectangle surface and fluid: ammonia		
Pitch (mm)	Outlet Temperature (K)	Effectiveness (%)
0.95	361.93	97.4
0.475	363	100
0.2375	363	100
0.11875	363	100

For triangle surface and fluid: Freon 113		
Pitch (mm)	Outlet Temperature (K)	Effectiveness (%)
0.95	360.467	93.97
0.475	362.93	99.83
0.2375	363	100
0.11875	363	100

For rectangle surface and fluid: Freon 113		
Pitch (mm)	Outlet Temperature (K)	Effectiveness (%)
0.95	361.53	96.5
0.475	363	100
0.2375	363	100
0.11875	363	100

For triangle surface and fluid: Freon 11		
Pitch (mm)	Outlet Temperature (K)	Effectiveness (%)
0.95	361.4	96.19
0.475	363	100
0.2375	363	100
0.11875	363	100

For rectangle surface and fluid: Freon 11		
Pitch (mm)	Outlet Temperature (K)	Effectiveness (%)
0.95	362.067	97.7
0.475	363	100
0.2375	363	100
0.11875	363	100

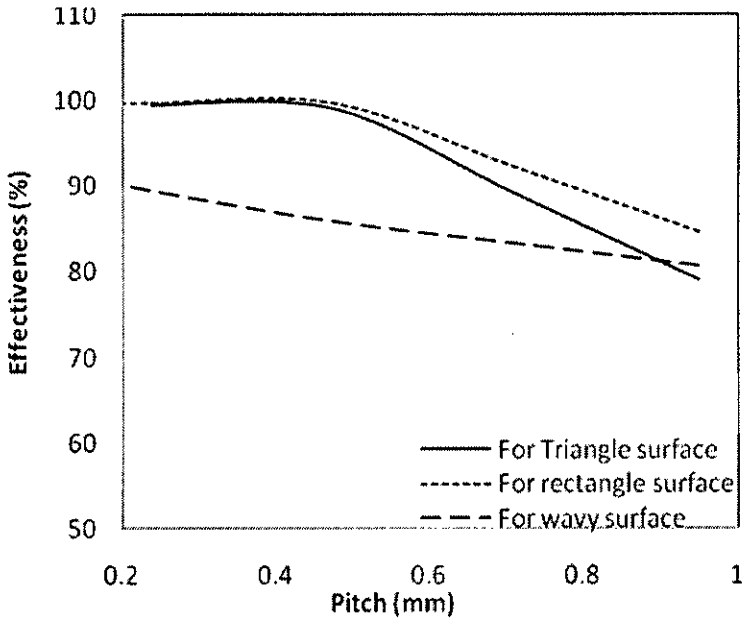

Figure 4.32 Comparison of Effectiveness of water with pitches for different geometry MEMS heat exchanger

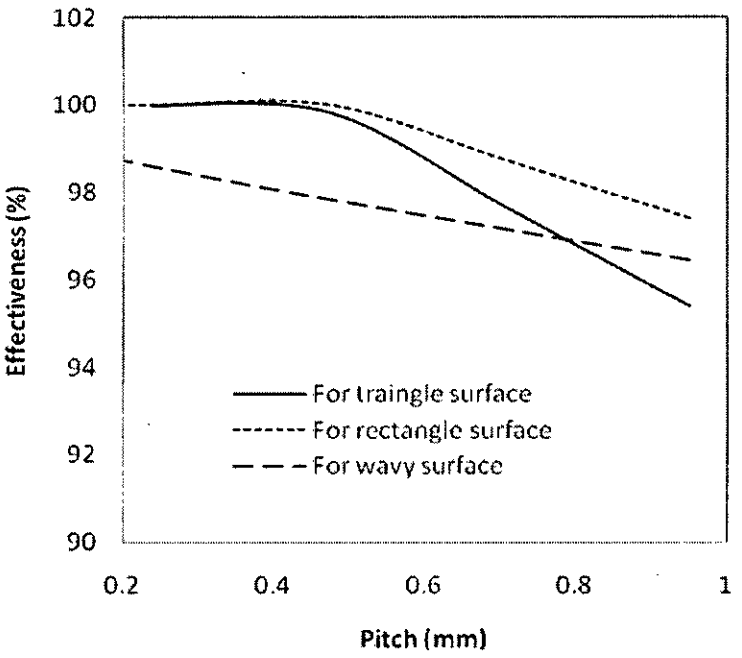

Figure 4.33 Comparison of Effectiveness of ammonia with pitches for different geometry MEMS heat exchanger

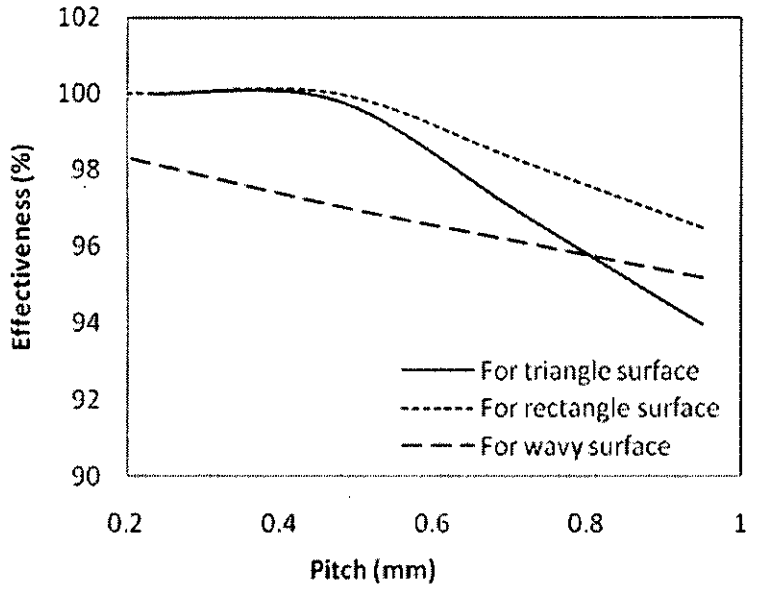

Figure 4.34 Comparison of Effectiveness of Freon 113 with pitches for different geometry MEMS heat exchanger

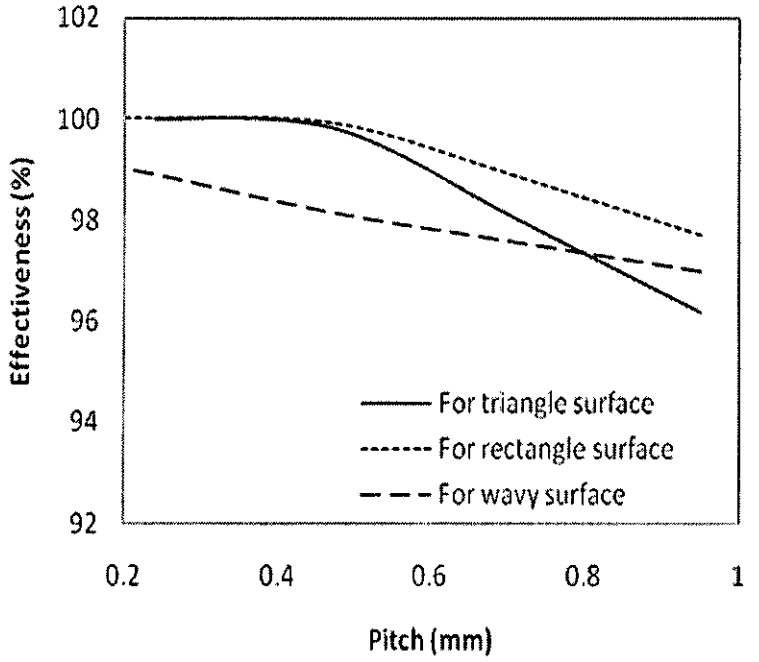

Figure 4.35 Comparison of Effectiveness of Freon 11 with pitches for different geometry MEMS heat exchanger

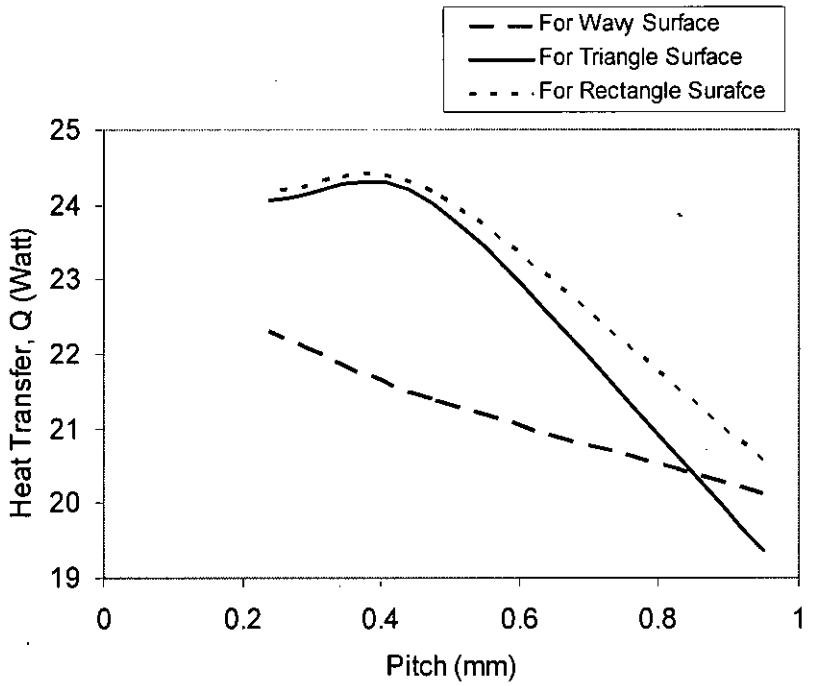

Figure 4.36 Comparison of heat transfer of water for different geometry of MEMS heat exchanger for Uav = 0.015 m/s

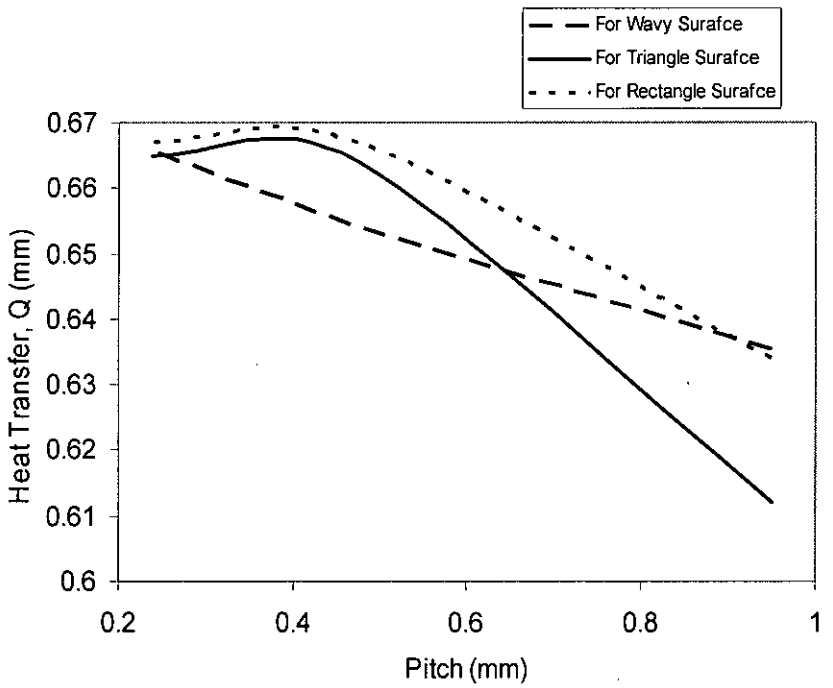

Figure 4.37 Comparison of heat transfer of ammonia for different geometry of MEMS heat exchanger for Uav = 0.015 m/s

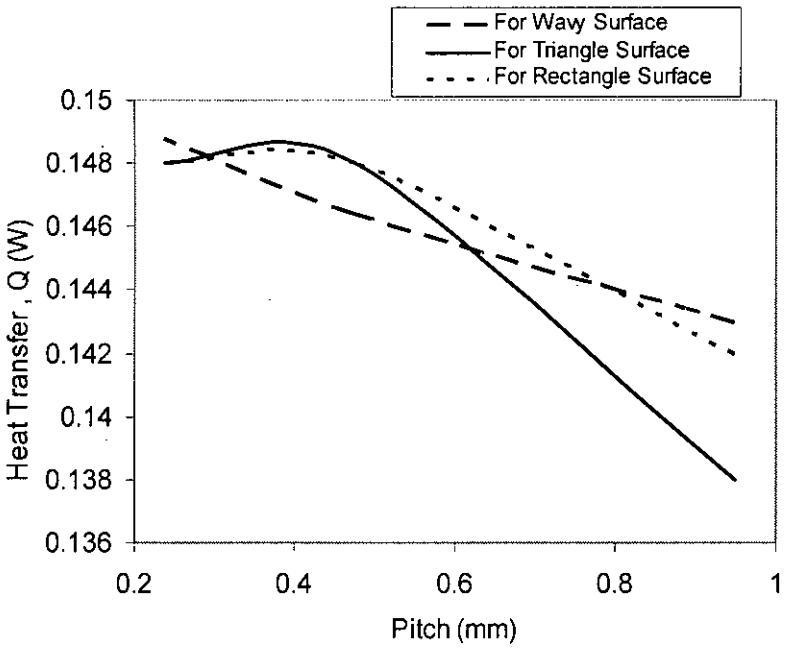

Figure 4.38 Comparison of heat transfer of Freon 11 for different geometry of MEMS heat exchanger for Uav = 0.015 m/s

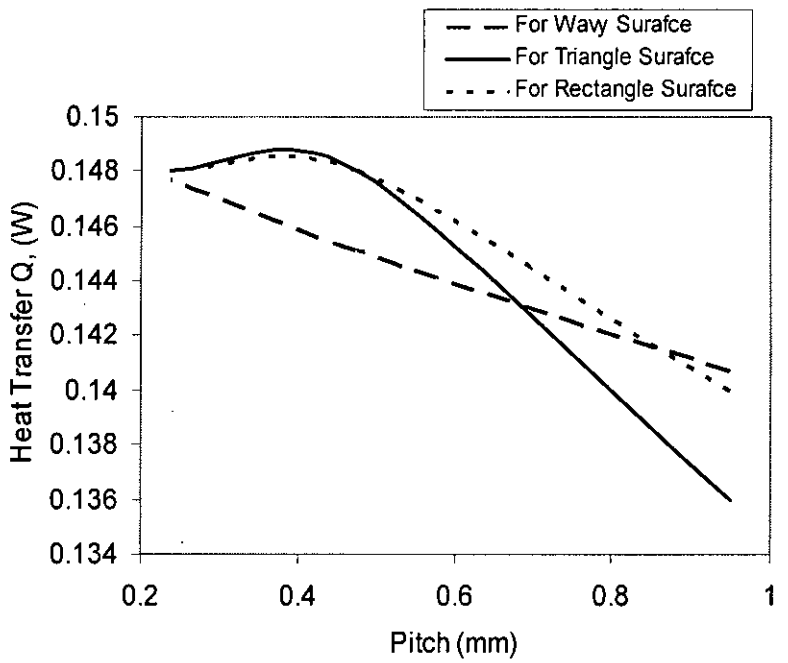

Figure 4.39 Comparison of heat transfer of Freon 113 for different geometry of MEMS heat exchanger for Uav = 0.015 m/s

4.7 Flow Pattern of Different Working Fluids for Triangular Surface

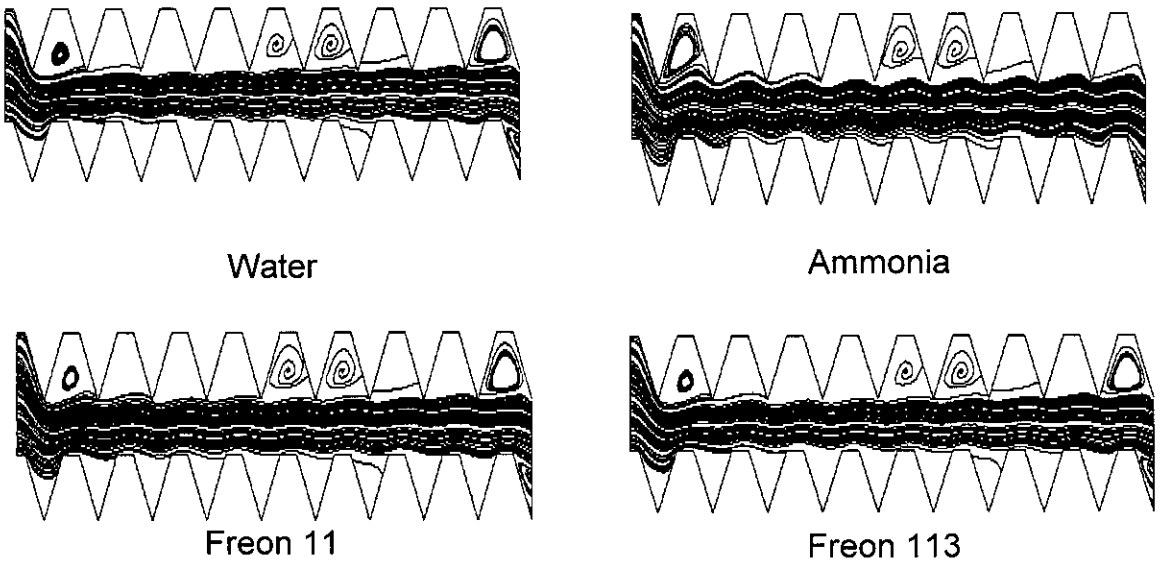

Figure 4.40 Flow patterns of different fluids for pitch 0.95 mm of triangle surface MEMS heat exchanger and Uav = 0.015 m/s

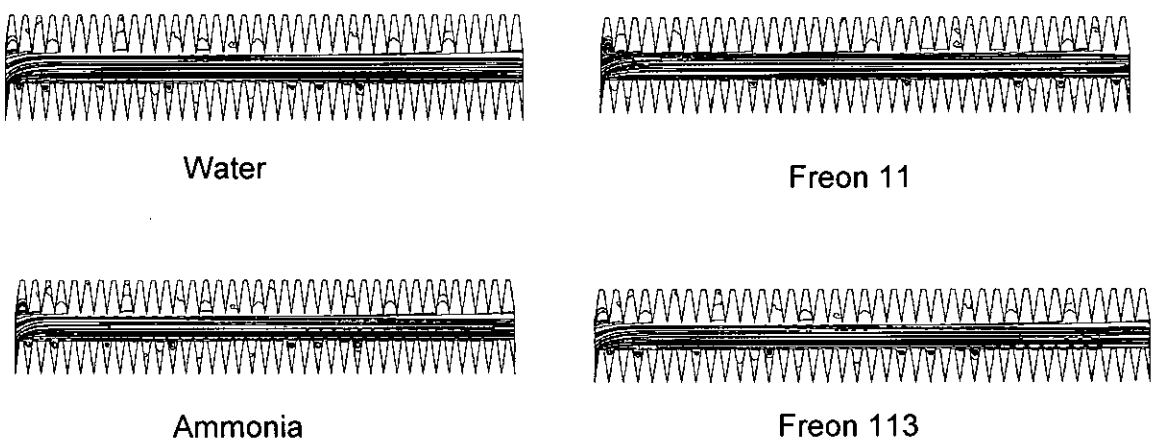

Figure 4.41 Flow patterns of different fluids for pitch 0.2375 mm of triangle surface MEMS heat exchanger and Uav = 0.015 m/s

4.8 Flow Pattern of Different Working Fluids for Rectangular Surface

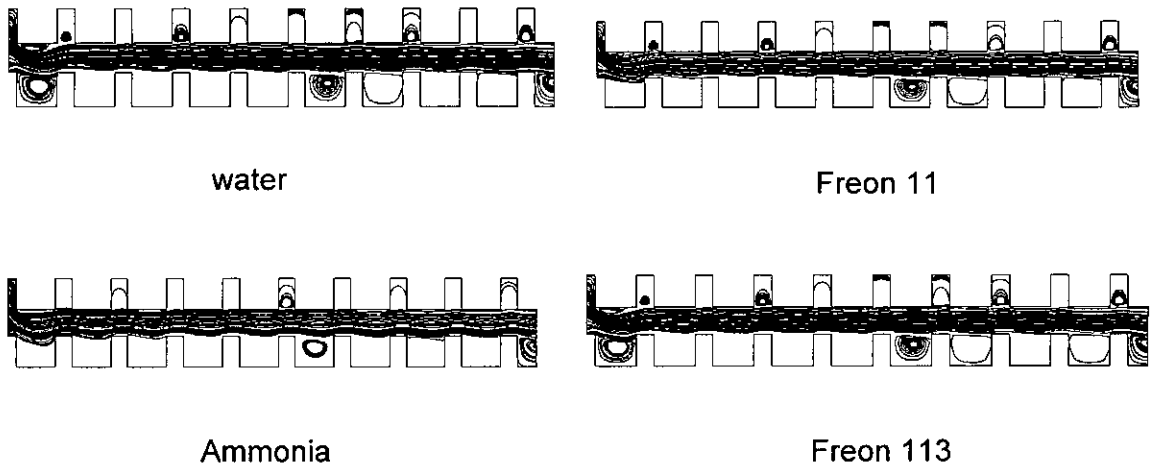

Figure 4.42 Flow patterns of different fluids for pitch 0.95 mm of rectangle surface MEMS heat exchanger and Uav = 0.015 m/s

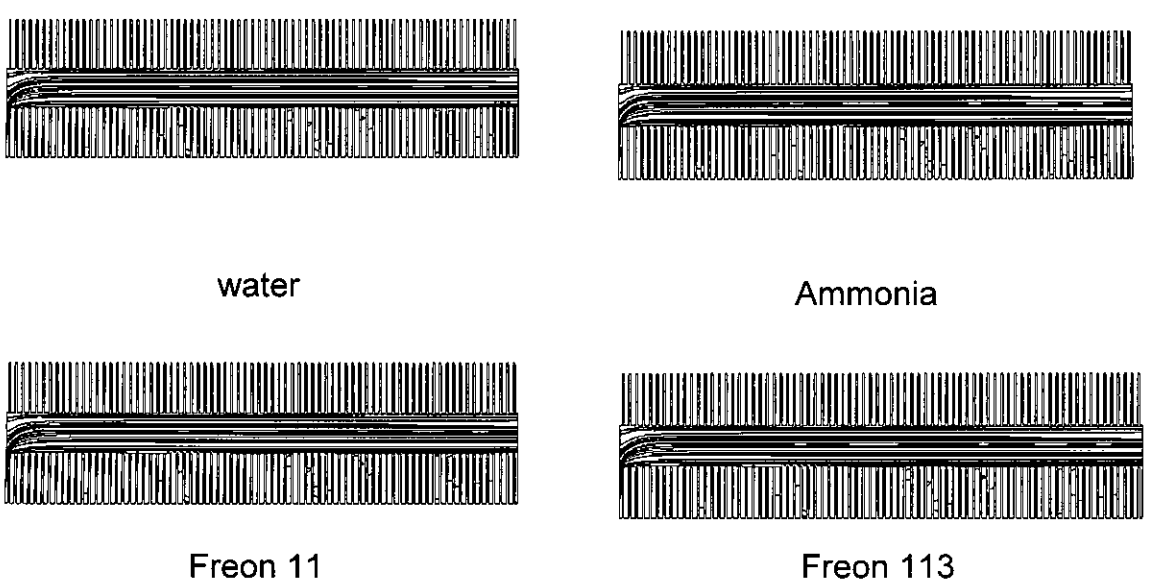

Figure 4.43 Flow patterns of different fluids for pitch 0.11875 mm of rectangle surface MEMS heat exchanger and Uav = 0.015 m/s

Figures 4.40 to 4.43 show velocity field for different fluids in triangular and rectangular surface MEMS heat exchanger. It is clear from the figures that for pitch length of 0.95 mm vortices form in the summit and hollow whereas if pitch is reduced no vortices is seen and straight streamlines are observed with no variation from one instant to the next.

4.9 Comparison of Refrigerants used in the Analysis for Different Geometry

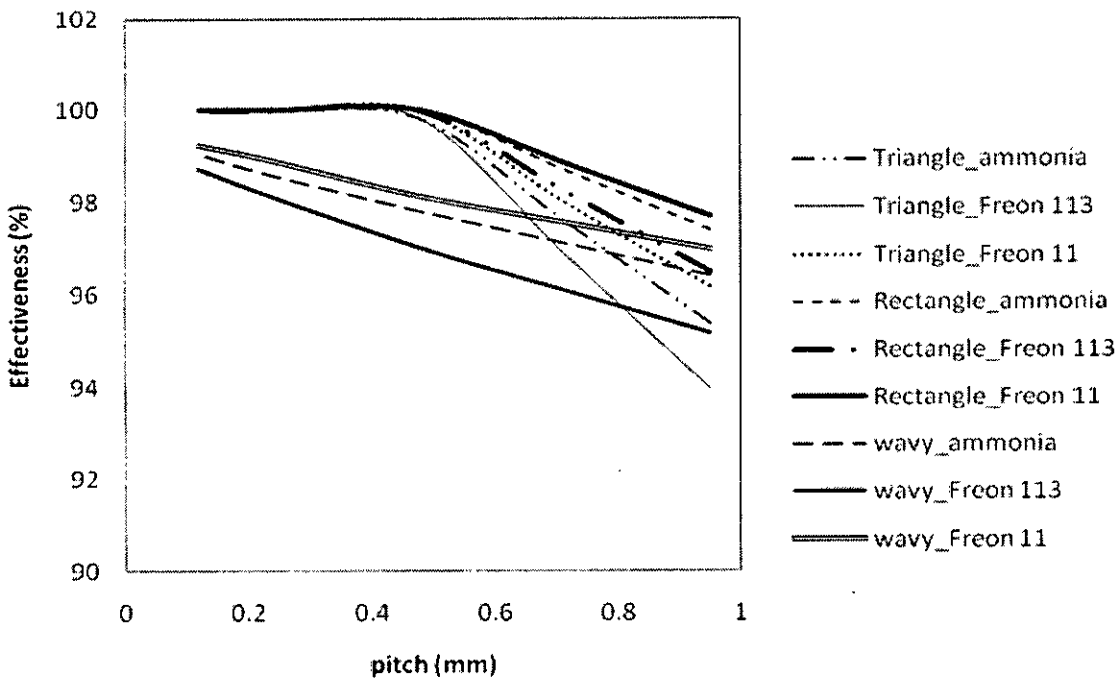

Figure 4.44 Comparison of effectiveness of different refrigerants for different geometry of MEMS heat exchanger for Uav = 0.015 m/s

The above figure shows comparison of performance in terms of effectiveness of refrigerants in different geometry. It shows clearly that rectangle surface with Freon 11 as working fluid shows highest effectiveness compared to other combinations. In case of less number of peaks the diminishing rate of the value of effectiveness is also the lowest for Freon 11 in MEMS heat exchanger with rectangular surface.

Chapter 5

Conclusion

5.1 Preamble

This study is an attempt to present the effect of different working fluids on heat transfer characteristics under steady state condition in a MEMS heat exchanger. Various investigations have been conducted earlier using air as working fluid. Most of the researches have been based on wavy shape, comparison with conventional heat exchangers and effect of different parameters on heat transfer rates. So it has become essential to compare its performance with others as other fluids may have some merits over air such as higher heat transfer rate, dust free content, low fluid pumping cost etc. It will be helpful for researchers if they may find substitutes of conventional working fluids. Air and water are mostly available fluid and inexpensive as working fluid. Availability and economy is of course a great issue while designing a MEMS heat exchanger. Water is cheap but has some disadvantages of forming rust on metals but despite of this demerit it is the most popular coolant used worldwide as its heat transfer rate is high. Again, by forcing the fluids through the heat exchanger at higher velocities the overall heat transfer coefficient may be increased (shown in Figure 4.5), but this higher velocity results in a larger pressure drop through the heat exchanger and correspondingly larger pumping costs. Besides these, there may be some constraints such as, not every fluid can be used for every condition. So a comparison of fluids is essential to evaluate their performance as working fluid in heat exchanger.

5.2 Conclusions

The following facts have been emerged from the present analysis.

1. MEMS heat exchanger is more effective at lower flow rate. The higher the Reynolds numbers the less the effectiveness. For an optimum value of Reynolds

number, Freon 11 exhibits the greatest effectiveness, which is 79%. The magnitude for Freon 113, ammonia, water and air are 72%, 77%, 67% and 64% respectively.

2. At higher velocities, the heat transfer coefficient increases. Water shows the highest value of heat transfer coefficient among the fluids considered here. The value also increases linearly with increase in velocity. On the contrary, heat transfer coefficient of other fluids increases slowly with the increase in Reynolds number.
3. Freon 11 shows the highest outlet mean temperature in comparison to other fluids when peak is increased for same wavy length. It means that it can transfer heat more effectively than other fluids.
4. Water shows highest value of heat transfer when compared to other fluids as its heat transfer coefficient is higher than others. For changing the pitch length from 0.95 mm to 0.11875 mm, water shows the highest value of increment of heat transfer which is 13.27 %, ammonia, Freon 113, Freon 11 shows increment of 5.4%, 5.7% and 4.5% respectively.
5. Increasing the peaks after reaching pitch 0.475 mm has no effect on effectiveness and heat transfer behaviour in case of triangular and rectangular surface.
6. Rectangular surface can be considered instead of wavy surface while designing MEMS heat exchanger as its performance is better than triangular and wavy surface and also easier to manufacture.

It may be concluded that water and air are the most widely used coolants for their easy availability. But the disadvantage of forming rust by water and containing dust in air can bar the way of using these fluids as coolant. The need of finding substitutes for these coolants may arise then. The aim of this analysis has been to find out an alternative working fluid for MEMS heat exchanger. After accomplishing this analysis, the fact is well established that refrigerants such as Freon 11, Freon 113 and ammonia can be used as heat transfer medium of MEMS heat exchangers for micro electro-mechanical systems. Moreover, cost effectiveness, ease of manufacture and better heat transfer

behaviour of geometry should be considered while designing MEMS heat exchangers. This work also suggests that rectangular surface can be used instead of other geometry for having these advantages over other geometries.

5.3 Recommendations

The numerical simulation presented here suggests the following recommendations. The researchers who will work on this analysis may start from these.

1. The analysis was considered for single phase flow of the working fluids. Two phase flow will extend this study to a more pragmatic level.
2. A three dimensional model may comprise of other parameters which might have been skipped here. 3D model can help to attain more accurate result.
3. This analysis has been limited for three working fluids as substitutes. But more fluids should be taken for consideration so that other options may come to the light.
4. Solution for unsteady condition may help to acquire data with time which is not done here.
5. Pressure drop characteristics and friction may be considered during calculation of different heat exchanger design parameters.
6. Analysis for keeping the refrigerants in liquid phase may help to find better result of heat transfer behaviour and thus may show a better substitute of conventional working fluids for MEMS heat exchanger.

References

[1] Yuen, W., and Hsu, I. C., "An Experimental Study and Numerical Simulation of Two-Phase Flow of Cryogenic Fluids through Micro-Channel Heat Exchanger," CRYOCOOLER 10, 10th International Cryocooler Conference, pp. 497-504, 1998.

[2] Hardt, S., Ehrfeld, W., Hessel, V. and Vanden Bussche, K. M., "Simulation of Heat-Transfer Enhancement Effects in Microreactors," Technical Proceedings of the International Conference on Modeling and Simulation of Microsystems, pp. 644 – 647, 2000.

[3] Okabe, T, Foli, K., Olhofer, M., Jin, Y., and Okabe, B. S., "Comparative Studies on Micro Heat Exchanger Optimisation," Vol. 1, pp. 647 – 654, 8-12 December. 2003.

[4] Hossain, M. Z., and Islam, A., K., M., S., "Numerical Investigation of Unsteady Flow and Heat Transfer in Wavy Channels," 15th Australasian Fluid Mechanics Conference, The University of Sydney, Sydney, Australia, 13-17 December 2004.

[5] Chandratilleke, T., Banney, B., and Clarke, P., "High Performance Heat Exchanger for Thermoelectric Cooling With Large Heat Loads," Proceedings of 23rd International Conference on Thermolectrics 2004 (ICT2004), University of South Australia, Adelaide, Australia, 25th-29th July 2004.

[6] McCandless, A., Motakef, S., Guidry, D., and Overholt, M., "Micro-structured Heat Exchangers and Reactors for ISRU and Energy Conversion," Space Resources Roundtable VI. LPI, Contribution No. 1224. Proceedings of the conference, Colorado School of Mines, Golden Colorado, USA pp. 32, November 1-3, 2004.

[7] Li, D., "Microfluidics in Lab-on-a-Chip: Models, Simulations and Experiments", in Microscale Heat Transfer- Fundamental and Applications, Kluwer Academic Publishers, the Netherlands, 2005.

[8] Morimoto, K., Suzuki, Y., and Kasagi, N., "Optimal Shape Design of Counter-Flow Primary Surface Recuperators," Proceedings of the Fifth International Conference on Enhanced, Compact and Ultra-Compact Heat Exchangers: Science, Engineering and Technology, NJ, USA, September 2005.

[9] Mébrouk, R., Abdellah, B., and Abdelkader, S., "Effect of Wall Waviness on Heat Transfer by Natural Convection in A Horizontal Wavy Enclosure," International Journal of Applied Engineering Research, Vol. 1 No. 2, pp. 187-201, 2006.

[10] Eiamsa-ard, S., and Promvonge, P., "Enhancement of Heat Transfer in a Circular Wavy-Surfaced Tube with a Helical-tape Insert," International Energy Journal, Vol. 8, Issue 1, March 2007.

[11] Davis, M., Weymouth, R., and Clarke, P., "Thermoelectric CPU Cooling using High Efficiency Liquid Flow Heat Exchangers," Proceedings of the COMSOL Users Conference, Taipei, 2007.

[12] Dunn, P., and Reay, D., A., "Heat Pipes," Second Edition, Pergamon Press Inc., NY, USA, pp. 294-296, 1978.

[13] Holman, J., P., "Heat Transfer", 8th Edition, McGraw-Hill Inc., USA, pp. 553-597., 1997.

[14] Khurmi, R., S., and Gupta, J., K., " A Textbook of Refrigeration and Air Conditioning," S. Chand & Company Ltd., New Delhi, India, 2003.

Appendix A

Fluid Properties

Temperature dependent properties of different fluids are taken from the following data tables:

AMMONIA

^{o}C	kJ/kg	kg/m^3	kg/m^3	$W/m^{o}C$	cP	$cPx10^2$	Bar	$kJ/kg^{o}C$	$N/mx10^2$
-60	1434	714.4	0.03	0.294	0.36	0.72	0.27	2.050	4.062
-40	1384	690.4	0.05	0.303	0.29	0.79	0.76	2.075	3.574
-20	1338	665.5	1.62	0.304	0.26	0.85	1.93	2.100	3.090
0	1263	638.6	3.48	0.298	0.25	0.92	4.24	2.125	2.480
20	1187	610.3	6.69	0.286	0.22	1.01	8.46	2.150	2.133
40	1101	579.5	12.00	0.272	0.20	1.16	15.34	2.160	1.833
60	1026	545.2	20.49	0.255	0.17	1.27	29.80	2.180	1.367
80	891	505.7	34.13	0.235	0.15	1.40	40.90	2.210	0.767
100	699	455.1	54.92	0.212	0.11	1.60	63.12	2.260	0.500
120	428	374.4	113.16	0.184	0.07	1.89	90.44	2.292	0.150

Source: Ref. [12]

FREON 11

Temp. °C	Latent Heat kJ/kg	Liquid Density kg/m^3	Vapour Density kg/m^3	Liquid Thermal Conductivity W/m^oC	Liquid Viscos. cP	Vapour Viscos. $cPx10^2$	Vapour Press. Bar	Vapour Specific Heat kJ/kg^oC	Liquid Surface Tension $N/mx10^2$
-60	211.9	1672	0.04	0.121	1.19	0.86	0.02	0.476	2.95
-40	204.0	1622	0.04	0.115	0.98	0.88	0.05	0.497	2.70
-20	196.8	1578	1.04	0.111	0.70	0.95	0.16	0.516	2.40
0	190.0	1533	2.59	0.108	0.55	1.01	0.42	0.532	2.18
20	183.4	1487	5.38	0.100	0.44	1.08	0.93	0.546	1.92
40	175.6	1439	10.07	0.097	0.37	1.14	1.82	0.561	1.66
60	167.5	1389	16.85	0.094	0.32	1.20	3.14	0.576	1.40
80	159.0	1334	30.56	0.089	0.28	1.25	5.85	0.590	1.14
100	146.9	1265	49.04	0.076	0.25	1.31	9.53	0.607	0.90
120	134.4	1194	67.53	0.064	0.23	1.37	13.21	0.623	0.63
140	117.0	1105	110.66	0.055	0.22	1.49	18.92	0.646	0.37

Source: Ref. [12]

FREON 113

Temp. °C	Latent Heat kJ/kg	Liquid Density kg/m^3	Vapour Density kg/m^3	Liquid Thermal Conductivity W/m^oC	Liquid Viscos. cP	Vapour Viscos. $cPx10^2$	Vapour Press. Bar	Vapour Specific Heat kJ/kg^oC	Liquid Surface Tension $N/mx10^2$
-50	173.0	1720	0.15	0.120	2.300	0.85	0.01	0.600	2.86
-30	167.8	1683	0.32	0.119	1.604	0.90	0.03	0.613	2.60
-20	165.4	1664	0.46	0.118	1.323	0.92	0.05	0.619	2.47
-10	163.2	1643	0.77	0.118	1.108	0.94	0.09	0.626	2.34
0	160.6	1621	1.26	0.117	0.942	0.97	0.12	0.632	2.21
10	158.0	1599	1.95	0.108	0.812	0.99	0.19	0.644	2.08
20	155.2	1576	3.00	0.098	0.707	1.02	0.37	0.656	1.96
30	152.3	1553	4.34	0.097	0.622	1.04	0.55	0.664	1.84
40	149.2	1529	6.02	0.095	0.553	1.07	0.79	0.669	1.73
50	145.9	1503	8.79	0.094	0.502	1.09	1.11	0.674	1.62
70	139.4	1452	14.34	0.091	0.401	1.13	2.04	0.691	1.40

Source: Ref. [12]

WATER

°F	°C	c_p, kJ/kg · °C	ρ, kg/m³	μ, kg/m · s	k, W/m · °C	Pr	$\frac{g\beta\rho^2 c_p}{\mu k}$, 1/m³ · °C
32	0	4.225	999.8	1.79×10^{-3}	0.566	13.25	
40	4.44	4.208	999.8	1.55	0.575	11.35	1.91×10^{9}
50	10	4.195	999.2	1.31	0.585	9.40	6.34×10^{9}
60	15.56	4.186	998.6	1.12	0.595	7.88	1.08×10^{10}
70	21.11	4.179	997.4	9.8×10^{-4}	0.604	6.76	1.46×10^{10}
80	26.67	4.179	995.8	8.6	0.614	5.85	1.91×10^{10}
90	32.22	4.174	994.9	7.65	0.623	5.12	2.48×10^{10}
100	37.78	4.174	993.0	6.82	0.630	4.53	3.3×10^{10}
110	43.33	4.174	990.6	6.16	0.637	4.04	4.19×10^{10}
120	48.89	4.174	988.8	5.62	0.644	3.64	4.89×10^{10}
130	54.44	4.179	985.7	5.13	0.649	3.30	5.66×10^{10}
140	60	4.179	983.3	4.71	0.654	3.01	6.48×10^{10}
150	65.56	4.183	980.3	4.3	0.659	2.73	7.62×10^{10}
160	71.11	4.186	977.3	4.01	0.665	2.53	8.84×10^{10}
170	76.67	4.191	973.7	3.72	0.668	2.33	9.85×10^{10}
180	82.22	4.195	970.2	3.47	0.673	2.16	1.09×10^{11}
190	87.78	4.199	966.7	3.27	0.675	2.03	
200	93.33	4.204	963.2	3.06	0.678	1.90	
220	104.4	4.216	955.1	2.67	0.684	1.66	
240	115.6	4.229	946.7	2.44	0.685	1.51	
260	126.7	4.250	937.2	2.19	0.685	1.36	
280	137.8	4.271	928.1	1.98	0.685	1.24	
300	148.9	4.296	918.0	1.86	0.684	1.17	
350	176.7	4.371	890.4	1.57	0.677	1.02	
400	204.4	4.467	859.4	1.36	0.665	1.00	
450	232.2	4.585	825.7	1.20	0.646	0.85	
500	260	4.731	785.2	1.07	0.616	0.83	
550	287.7	5.024	735.5	9.51×10^{-5}			
600	315.6	5.703	678.7	8.68			

Source: Ref. [13]

AIR

T, K	ρ, kg/m³	c_p, kJ/kg·°C	$\mu \times 10^6$, kg/m·s	$\nu \times 10^6$, m²/s	k, W/m·°C	$\alpha \times 10^6$, m²/s	Pr
100	3.6010	1.0266	0.6924	1.923	0.009246	0.02501	0.770
150	2.3675	1.0099	1.0283	4.343	0.013735	0.05745	0.753
200	1.7684	1.0061	1.3289	7.490	0.01809	0.10165	0.739
250	1.4128	1.0053	1.5990	11.31	0.02227	0.15675	0.722
300	1.1774	1.0057	1.8462	15.69	0.02624	0.22160	0.708
350	0.9980	1.0090	2.075	20.76	0.03003	0.2983	0.697
400	0.8826	1.0140	2.286	25.90	0.03365	0.3760	0.689
450	0.7833	1.0207	2.484	31.71	0.03707	0.4722	0.683
500	0.7048	1.0295	2.671	37.90	0.04038	0.5564	0.680
550	0.6423	1.0392	2.848	44.34	0.04360	0.6532	0.680
600	0.5879	1.0551	3.018	51.34	0.04659	0.7512	0.680
650	0.5430	1.0635	3.177	58.51	0.04953	0.8578	0.682
700	0.5030	1.0752	3.332	66.25	0.05230	0.9872	0.684
750	0.4709	1.0856	3.481	73.91	0.05509	1.0774	0.686
800	0.4405	1.0978	3.625	82.29	0.05779	1.1951	0.689
850	0.4149	1.1095	3.765	90.75	0.06028	1.3097	0.692
900	0.3925	1.1212	3.899	99.3	0.06279	1.4271	0.696
950	0.3716	1.1321	4.023	108.2	0.06525	1.5510	0.699
1000	0.3524	1.1417	4.152	117.8	0.06752	1.6779	0.702
1100	0.3204	1.160	4.44	138.6	0.0732	1.969	0.704
1200	0.2947	1.179	4.69	159.1	0.0782	2.251	0.707
1300	0.2707	1.197	4.93	182.1	0.0837	2.583	0.705
1400	0.2515	1.214	5.17	205.5	0.0891	2.930	0.705
1500	0.2355	1.230	5.40	229.1	0.0946	3.262	0.705
1600	0.2211	1.248	5.63	254.5	0.100	3.609	0.705
1700	0.2092	1.26.	5.85	280.5	0.106	3.977	0.705
1800	0.1970	1.267	6.07	308.1	0.111	4.379	0.704
1900	0.1858	1.309	6.29	338.5	0.117	4.811	0.704
2000	0.1762	1.338	6.50	369.0	0.124	5.260	0.702
2100	0.1682	1.372	6.72	399.6	0.131	5.713	0.700
2200	0.1602	1.419	6.93	432.6	0.139	6.120	0.707
2300	0.1538	1.482	7.14	464.0	0.149	6.540	0.710
2400	0.1458	1.574	7.35	504.0	0.161	7.020	0.718
2500	0.1394	1.688	7.57	543.5	0.175	7.448	0.730

Source: Ref. [13]

Appendix B

Procedure of Modeling of MEMS heat exchanger in FEMLAB 3.0

After entering variable names in the Constants dialog box and expressions of fluid properties such as dynamic viscosity, specific heat at constant pressure, density and thermal conductivity in the Subdomain Expressions dialog box under the Options menu, grid settings has been adjusted to draw the desired geometry of MEMS heat exchanger.

Geometry Modeling

Wavy Surface Pitch length 0.95 mm

1. To double click on the SOLID field in the status bar to clear the solidification option. This enables to create open ended line segments.
2. To click the 2nd Degree Bezier Curve button and click on the points (0, 0.7e-3), (0.15e-3, 1e-3) and (.3e-3, 0.7e-3).
3. To click on Line button in order to draw a straight line from (.3e-3, 0.7e-3) to (.5e-3, 0.3e-3). To right-click to terminate the line. To draw a second Bezier curve through the points (.5e-3, 0.3e-3), (0.65e-3, 0) and (0.8e-3, 0.30e-3).
4. To finish by drawing a line through (0.8e-3, 0.30e-3), (1e-3, 0.70e-3).
5. To press Ctrl+A in order to select all segments. To click the Array button on the draw toolbar. On the Rectangular tab, to specify the following values.

Component	Displacement	Array Size
x	1e-3	10
y	-1e-3	2

6. To click OK.

7. To open the Axes/Grid Settings dialog box under the Options menu. On the Axis tab, to select the Axis equal check box and on the Grid tab, to clear the Auto check box and to type 5e-5 in the x-spacing and y-spacing edit fields. To type space separated 1.5e-4 0.00965 in the Extra x edit field and space separated -9e-4 -2.5e-4 3e-4 8.5e-4 in the Extra y edit field. To click OK and to click the Zoom Window button and to zoom in on the leftmost few bends of the heat exchanger.
8. To select the line button and draw two straight Lines, one from (1.5e-4, 8.5e-4) to (1.5e-4, -2.5e-4). To zoom out and in on the right portion of the geometry and to draw the other line from (9.65e-3, 0.3e-3) to (9.65e-3, -0.9e-3).
9. To press Ctrl+A to select all segments and to click the Coerce to Solid button on the left toolbar.
10. To click the Zoom Extents button.

Physics Settings

Boundary Conditions

1. To choose Incompressible Navier-Stokes (ns) from the Multiphysics menu. In the Boundary Conditions, to select inlet boundary (for wavy surface Pitch length 0.95 mm boundary 1) and Inflow/Outflow velocity from the list. To set the parabolic velocity profile by typing Uav*6*s*(1-s) in the u_0 edit field.
2. To select Normal flow/Pressure condition for outlet boundary (boundary 40 for wavy surface Pitch length 0.95 mm) for wavy surface, and to set p_0 to 0.
3. To click OK.

Subdomain Settings

1. To enter material properties in all the subdomains in the Subdomain Settings dialog box under the Physics menu.
2. To switch to the Init tab and to enter Uav for the u (t^0) initial value. To click OK.

Boundary Conditions

1. To switch to the Convection and Conduction (cc) application mode.
2. To open the Boundary Settings dialog box from the Physics menu and to specify the boundary conditions.
3. To click OK.

Boundary	Inlet	Others	Outlet
Conditions	Temperature T_{in}	Temperature T_h	Convective Flux

Subdomain Settings

1. To open the Subdomain Settings dialog box from the Physics menu and to specify material properties.
2. To select the Artificial Stabilization check box and to select the Streamline Diffusion check box with default settings.
3. To switch to the Init tab and to enter T_h for the $T(t^0)$ initial value.
4. To click OK.

Mesh Generation

1. To select Mesh Parameters from the Mesh menu and select Fine in the Predefined mesh sizes list.
2. To select the Boundary tab and to select inlet and outlet boundaries (boundaries 1 and 40 for wavy surface Pitch length 0.95 mm). To type 2e-5 in the Maximum element size edit field.
3. To click OK.
4. To click Initialize Mesh in the Main toolbar.

Computing the Solution

To solve the problem by pressing the Solve Problem button in the Main toolbar.

Determination of Outlet Mean Temperature

The default plot is the temperature field. Steps for calculation of outlet mean temperature are as follows:

1. In the Postprocessing menu, to select Boundary Integration and then to select outlet boundary and to type T*u in the Expression edit field. To click OK. The value appears in the message log.
2. To Repeat the procedure, but this time to select x-velocity (ns) in the Predefined quantities drop down list. To divide the first value with the second.

Geometry Modeling for Other Surfaces

The procedure which has been followed for modeling of other shapes of MEMS heat exchanger is quite similar with that of wavy surface. In case of pitch length of 0.95 mm for triangular and rectangular surface heat exchanger, straight lines have been drawn instead of curves and Bezier Curve button has not been used. For varying the pitch, number of peaks for the total length has been varied as 19, 38 and 76 to obtain pitch length of 0.475mm, 0.2375 mm and 0.11875 mm respectively.